

Energy Efficient SWIPT: From Fully-Digital to Hybrid Analog-Digital Beamforming

Ang Li, *Student Member, IEEE*, and Christos Masouros, *Senior Member, IEEE*

Abstract—Simultaneous wireless information and power transfer (SWIPT) enables the transmission of information symbols and energy simultaneously. In this paper, we study the MIMO SWIPT systems with limited RF chains at the base station. We focus on the scenario where there is one information decoder with a target SINR and several separate energy harvesting receivers with harvested energy thresholds. To motivate our energy-efficient hybrid analog-digital beamforming strategy, the fully-digital power minimization problem is firstly analyzed, where we mathematically show that the optimal beamformer consists of only the information beamformer, and derive closed-form beamformers for a number of special cases. Based on this result, we further consider hybrid beamforming and propose an iterative scheme where the analog and digital beamformers are alternately updated. For the proposed scheme, in each iteration we design the analog beamformer by minimizing the difference between the fully-digital beamformer and the hybrid beamformer. Based on our above analysis for fully-digital case, the optimal solution for analog beamformer can be obtained via a geometrical interpretation. We further design the robust beamformers for the proposed schemes, when only imperfect channel state information (CSI) is available. The numerical results show that the proposed iterative designs achieve a close-to-optimal performance with significant gains in the total power consumption over fully-digital SWIPT.

Index Terms—MIMO, SWIPT, hybrid beamforming, optimization, Lagrangian, geometrical approach.

I. INTRODUCTION

WITH the increasing traffic demand and number of user equipments (UEs) in the wireless environment, the power consumption of both the base stations (BSs) and UEs in the wireless communication systems has increased dramatically [1][2]. However, most UEs only have limited power supplies (batteries) currently, which has become a bottleneck when the power consumption is high, and the development of battery techniques cannot satisfy the current energy requirement [3]. Towards this direction, energy harvesting (EH) techniques have been proposed to exploit the natural energy such as solar, tide and wind to prolong the battery

life of UEs [4]. However, such techniques usually depend on the environmental conditions and the natural energy may not always be available, especially for the indoor environments. Recent advances have shown that electromagnetic (EM) radiation can be exploited as a potential energy source, based on the fact that EM waves convey energy that can be converted to direct current (DC) voltage with rectenna circuits [5][6]. A step further has been obtained by the wireless power transfer technique, which has been extensively studied for wireless sensor networks [7]-[9].

Similarly for wireless communications, the energy harvesting techniques and wireless power transfer enable the UEs to harvest energy from the EM waves in the communication links, and therefore have become particularly appealing [10]-[13]. For wireless communication systems, the RF signals carry both the information and energy at the same time, and there exists a fundamental tradeoff between information decoding and energy harvesting, which has been studied in [12] for flat fading and [13] for selective fading, respectively. Nevertheless, in [12][13] an ideal receiver that can simultaneously decode information and harvest energy with the same received signal is assumed, which is not applicable currently. Therefore, a more practical approach termed as simultaneously wireless information and power transfer (SWIPT) is considered in [14], where three different types of receivers are proposed, i.e. separate, time-switching and power-splitting. SWIPT with multiple-input-multiple-output (MIMO) techniques has subsequently attracted a lot of attention [15]-[19], where the SWIPT techniques for cellular networks are considered in [16][17]. In [18], a robust precoder for MIMO SWIPT systems for stochastic Rician fading is proposed. [19] employs the zero-forcing (ZF) method for MIMO SWIPT systems, where it is shown that the harvested energy obtained by the EH receivers can be increased at the cost of a signal-to-interference-plus-noise-ratio (SINR) loss of the information decoders (IDs). A harvested energy maximization beamforming for EH receivers while guaranteeing the SINR target of the IDs is considered in [20]. A data-aided transmit beamforming that exploits the constructive interference is proposed in [21], which further improves the performance of MIMO SWIPT systems. In [22]-[25], the joint information and energy beamforming methods are investigated for MIMO interference channels, while the applications of SWIPT techniques have been considered for interference alignment networks in [26]-[28]. By considering the broadcast nature of the wireless communications, SWIPT techniques have also been combined with physical layer security in [29]-[32].

In addition to the SWIPT techniques, energy-efficient trans-

Manuscript received September 05, 2017; revised November 13, 2017; accepted December 07, 2017. The associate editor coordinating the review of this paper and approving it for publication was Prof. Y. Li. (*Corresponding author: Ang Li.*)

Copyright (c) 2015 IEEE. Personal use of this material is permitted. However, permission to use this material for any other purposes must be obtained from the IEEE by sending a request to pubs-permissions@ieee.org.

A. Li and C. Masouros are with the Dept. of Electronic and Electrical Eng., University College London, Torrington Place, London, WC1E 7JE, UK (e-mail: ang.li.14@ucl.ac.uk, c.masouros@ucl.ac.uk).

This work was supported by the Royal Academy of Engineering, UK, the Engineering and Physical Sciences Research Council (EPSRC) project EP/M014150/1 and the China Scholarship Council (CSC).

mission is another way to manage the increasing power consumption of the wireless industry. The above existing designs for MIMO SWIPT systems [15]-[32] all assume a fully-digital beamformer, which requires a dedicated radio frequency (RF) chain for each antenna element. Such fully-digital designs will result in a high power consumption at the BS. Even with moderate numbers of antennas, the power consumption of the RF chains is dominant, and techniques that allow a reduction in the RF chains are desirable. To address this and achieve an energy-efficient transmission, hybrid beamforming schemes have been proposed for MIMO systems, which provide a key solution by allowing a reduced number of RF chains, and the beamforming is divided into the analog and digital domain [33]-[37]. In the analog domain, phase shifters are applied to provide high-dimensional phase-only controls, while a low-dimensional fully-digital beamformer is applied in the digital domain. Accordingly, the required number of RF chains is greatly reduced, which leads to a significant reduction in the total power consumption at the BS. It has been shown that the hybrid beamforming approaches can achieve a performance close to the fully-digital scheme, for both single-user case [33] and multi-user case [34]. However, the close-to-optimal performance is achieved by assuming a fully-connected structure for the antenna array, where each antenna element is connected to all RF chains. This structure requires a large number of combiners and phase shifters, which will introduce significant insertion losses in practice [38]-[40]. The hybrid beamforming techniques that take the specific practical losses into consideration have been studied in [38][39], where it is shown that a partially-connected structure is more preferable in practical implementation [40]. For the partially-connected structures, each antenna element is only connected to one RF chain. While the hybrid beamforming is initially proposed for massive MIMO systems, what has been neglected in the existing literature is that the hybrid structure is a promising candidate for energy-efficient transmission, which meets the requirement for the future wireless communication systems. Moreover, the reduction in the hardware complexity and power consumption directly applies to small-scale MIMO systems. Indeed, small access points (APs) for the future internet of things (IoTs) or small BSs (for example femtocells or picocells that are widely deployed for heterogeneous networks) usually have limited power supply, which can benefit from the hybrid structures. Interestingly, such power-efficient approaches by hybrid beamforming have yet to be explored for SWIPT.

Accordingly, in this paper we investigate the SWIPT techniques for small-scale MIMO systems with limited RF chains, where we study the scenario where the BS serves one ID and several EH receivers simultaneously. Specifically, we focus on the minimization of the required transmit power at the BS, while meeting the SINR requirement of the ID and the harvested energy requirement of each EH receiver. We firstly mathematically analyze the fully-digital beamforming problem with Lagrangian and Karush-Kuhn-Tucker (KKT) conditions, where we analytically show that the optimality is achieved by employing the information beamformer only. Particularly, for the case where there is only one EH receiver, we obtain the closed-form expressions of the optimal beamforming vectors.

We extend our study to the hybrid case, where we firstly propose a low-complexity hybrid scheme as a performance benchmark. In the low-complexity method, the analog beamformers are obtained based on the singular value decomposition (SVD) of the channel, and the low-dimensional digital beamformer is subsequently optimized based on the effective analog channel. To improve upon the above hybrid approach, the design of an iterative scheme is further introduced, where in each iteration we design the analog beamformer by minimizing the Euclidean distance between the fully-digital beamformer and the hybrid beamformer. Based on our analyses for the fully-digital case, the optimal analog beamformer can be efficiently solved via a geometrical interpretation. The extension to partially-connected structures at the BS is also introduced. Moreover, with the consideration that only imperfect channel state information (CSI) is available in practical systems, we further propose the robust hybrid beamforming scheme, where the channel uncertainties are addressed in the digital domain. The numerical results show that the proposed iterative scheme achieves a near-optimal performance for fully-connected structures, and the performance gains over the hybrid scheme based on SVD are more significant for partially-connected structures. It is also observed that the hybrid structures require a much less total power at the BS to achieve the same performance as the fully-digital structure, which verifies that the hybrid structures are more favourable for the future energy-efficient transmission.

For reasons of clarity, we summarize the contributions of this paper as:

- 1) We mathematically prove in Section III that it is optimal to employ only an information beamformer for the considered MIMO SWIPT systems. Specifically, we obtain the closed-form expressions for the special case of one ID and one EH receiver.
- 2) We extend our study to the hybrid structures with a limited number of RF chains. Two hybrid beamforming methods are proposed, where a low-complexity hybrid approach based on SVD is first presented in Section IV.
- 3) We further propose an iterative hybrid scheme in Section V, where the analog beamformer is designed by minimizing the Euclidean distance between the hybrid beamformer and the optimal fully-digital beamformer. Within each iteration, the optimal analog beamformer is obtained via a geometrical approach.
- 4) We investigate the case when only imperfect CSI is available in Section VI. We propose the robust hybrid scheme based on \mathcal{S} -procedure by considering the channel uncertainty in the digital domain.

The remainder of this paper is organized as follows. Section II presents the system model and conventional fully-digital SWIPT, followed by the analyses in Section III. The low-complexity hybrid scheme and iterative hybrid scheme are introduced in Section IV and V, respectively. In Section VI, we propose the robust hybrid beamforming for imperfect CSI. The numerical results are presented in Section VII where the power consumption model is included. This paper is concluded in Section VIII.

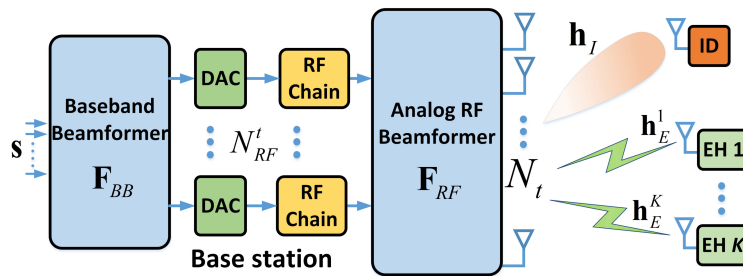


Fig. 1: Block diagram of the system model

Notations: a , \mathbf{a} , and \mathbf{A} denote scalar, vector and matrix, respectively. $\mathbb{E}\{\cdot\}$, $(\cdot)^T$, $(\cdot)^H$, $\text{rank}(\cdot)$, and $\text{tr}\{\cdot\}$ denote expectation, transposition, conjugate transposition, rank and trace of a matrix respectively. $|\cdot|$ and $\|\cdot\|$ denote the modulus and the Frobenius norm respectively, and \mathbf{I} is the identity matrix. We denote $\mathbf{0}$ as a zero matrix or vector. $\mathcal{C}^{n \times n}$ represents an $n \times n$ matrix in the complex set, and $\text{diag}(\cdot)$ denotes the conversion of a vector into a diagonal matrix. $[\mathbf{R}]_{m,n}$ denotes the element of the m th row and n th column in \mathbf{R} , and $\mathbf{R} \succeq 0$ means that \mathbf{R} is a Hermitian positive semidefinite matrix. $\Im\{a\}$ denotes the imaginary part of a complex variable a .

II. SYSTEM MODEL AND FULLY-DIGITAL SWIPT

We consider a downlink MIMO system as shown in Fig. 1, where a BS with N_t antennas and N_{RF}^t RF chains serves one single-antenna ID and K single-antenna EH receivers simultaneously. Perfect CSI is first assumed, while we investigate the case with imperfect CSI in Section VI. A spatially-uncorrelated flat-fading Rayleigh MIMO channel is assumed, and we denote $\mathbf{h}_I \in \mathcal{C}^{1 \times N_t}$ and $\mathbf{h}_E^k \in \mathcal{C}^{1 \times N_t}$ as the channel from the BS to the ID and EH receiver k , respectively. Each entry of \mathbf{h}_I and \mathbf{h}_E^k is modelled as [41]

$$\begin{aligned} [\mathbf{h}_I]_m &= \sqrt{\alpha_0 D_I^{-\beta} C_I} \cdot [\mathbf{g}_I]_m, \quad m \in \mathcal{M}, \\ [\mathbf{h}_E^k]_m &= \sqrt{\alpha_0 (D_E^k)^{-\beta} C_E^k} \cdot [\mathbf{g}_E^k]_m, \quad m \in \mathcal{M}, \end{aligned} \quad (1)$$

where we denote $\mathcal{M} = \{1, 2, \dots, N_t\}$. In (1), α_0 is a constant determined by the wireless propagation environment, D_I is the distance between the BS and the ID, β represents the pathloss coefficient, and C_I denotes the shadow fading. Each element of \mathbf{g}_I is independent and follows the standard complex Gaussian distribution, which forms the Rayleigh component of the channel. The denotation is similar for each \mathbf{h}_E^k of the EH receiver k .

When a conventional fully-digital beamforming scheme is applied, $N_{RF}^t = N_t$ and we denote the corresponding fully-digital beamforming matrix as $\mathbf{W} = [\mathbf{w}_I, \mathbf{w}_E^1, \dots, \mathbf{w}_E^K]$. Subsequently, we can express the received symbol at the ID as

$$r_I = \mathbf{h}_I \mathbf{w}_I s_I + \mathbf{h}_I \sum_{i=1}^K \mathbf{w}_E^i s_E^i + n_I, \quad (2)$$

where s_I and each s_E^i denote the data symbol. n_I represents the additive circular symmetric Gaussian noise with zero mean

and variance σ^2 . Following the existing literature [20], [22]-[25], we assume Gaussian signalling and express the received SINR for the ID as

$$\gamma_I = \frac{|\mathbf{h}_I \mathbf{w}_I|^2}{\sum_{k=1}^K |\mathbf{h}_I \mathbf{w}_E^k|^2 + \sigma^2}. \quad (3)$$

For the EH receivers, we assume the noise power at each receiver is the same as that of ID. For simplicity, a linear energy harvesting model as in [20]-[25], [42] is considered, and we express the harvested energy for the k -th EH receiver as

$$E_k = \eta \left(|\mathbf{h}_E^k \mathbf{w}_I|^2 + \sum_{i=1}^K |\mathbf{h}_E^k \mathbf{w}_E^i|^2 + \sigma^2 \right), \quad (4)$$

where η is a constant that represents the efficiency of converting the received radio signals into electrical energy. In (4), $0 < \eta < 1$ and for simplicity we have assumed that each EH receiver k has an identical energy transformation efficiency η .

We consider the optimization problem where the transmit power is minimized while meeting the SINR requirement of the ID and the harvested energy requirement of each EH receiver, which can be formulated as [21]

$$\begin{aligned} \mathcal{P}_1 : \quad & \min_{\mathbf{w}_I, \mathbf{w}_E^i} p \\ \text{s.t.} \quad & p \geq \|\mathbf{w}_I\|^2 + \sum_{i=1}^K \|\mathbf{w}_E^i\|^2 \end{aligned} \quad (5)$$

$$\begin{aligned} \gamma_I &\geq \gamma_0 \\ E_k &\geq E_0, \quad \forall k \in \mathcal{K} \end{aligned}$$

where $\mathcal{K} = \{1, 2, \dots, K\}$, and γ_0 is the SINR requirement of the ID. For simplicity we have assumed an identical harvested energy requirement for each EH receiver, which is denoted as E_0 .

III. ANALYSIS OF THE FULLY-DIGITAL BEAMFORMING PROBLEM AND CLOSED-FORM SOLUTIONS

To introduce the rationale behind the proposed hybrid iterative scheme in Section V, we firstly perform mathematical analyses on the fully-digital beamforming problem \mathcal{P}_1 with Lagrangian and KKT conditions, where we show that the optimality is achieved by employing the information beamformer only. While the KKT conditions are only necessary conditions for non-convex optimization problems, for the considered problems we can verify that the obtained solutions are also

sufficient. Similar conclusions can be drawn for the hybrid scheme, and these two observations motivate the design of the proposed iterative scheme in Section V.

A. A Special Case: Only One EH Receiver

We first consider a special case where there is one ID and one EH receiver in the system, which motivates the analyses for the case of $K > 1$ EH receivers and further the proposition of the optimal analog beamformer design in Section V. In this case \mathcal{P}_1 can be simplified as

$$\begin{aligned} \mathcal{P}_2 : \quad & \min_{\mathbf{w}_I, \mathbf{w}_E} \mathbf{w}_I^H \mathbf{w}_I + \mathbf{w}_E^H \mathbf{w}_E \\ \text{s.t.} \quad & \mathbf{h}_I \mathbf{w}_E \mathbf{w}_E^H \mathbf{h}_I^H + \sigma^2 - \frac{1}{\gamma_0} \mathbf{h}_I \mathbf{w}_I \mathbf{w}_I^H \mathbf{h}_I^H \leq 0 \quad (6) \\ & \frac{E_0}{\eta} - \sigma^2 - \mathbf{h}_E \mathbf{w}_E \mathbf{w}_E^H \mathbf{h}_E^H - \mathbf{h}_E \mathbf{w}_I \mathbf{w}_I^H \mathbf{h}_E^H \leq 0 \end{aligned}$$

Accordingly, we express the Lagrangian of \mathcal{P}_2 as [43]

$$\begin{aligned} \mathcal{L}(\mathbf{w}_I, \mathbf{w}_E, \lambda_I, \lambda_E) &= \mathbf{w}_I^H \mathbf{w}_I + \mathbf{w}_E^H \mathbf{w}_E \\ &+ \lambda_I \left(\mathbf{h}_I \mathbf{w}_E \mathbf{w}_E^H \mathbf{h}_I^H + \sigma^2 - \frac{1}{\gamma_0} \mathbf{h}_I \mathbf{w}_I \mathbf{w}_I^H \mathbf{h}_I^H \right) \quad (7) \\ &+ \lambda_E \left(\frac{E_0}{\eta} - \sigma^2 - \mathbf{h}_E \mathbf{w}_E \mathbf{w}_E^H \mathbf{h}_E^H - \mathbf{h}_E \mathbf{w}_I \mathbf{w}_I^H \mathbf{h}_E^H \right), \end{aligned}$$

where λ_I and λ_E denote the dual variables with respect to the SINR and harvested energy constraint, respectively. The KKT conditions for optimality are then obtained as

$$\frac{\partial \mathcal{L}}{\partial \mathbf{w}_I} = \mathbf{w}_I^H - \frac{\lambda_I}{\gamma_0} \mathbf{w}_I^H \mathbf{h}_I^H \mathbf{h}_I - \lambda_E \mathbf{w}_I^H \mathbf{h}_E^H \mathbf{h}_E = \mathbf{0} \quad (8a)$$

$$\frac{\partial \mathcal{L}}{\partial \mathbf{w}_E} = \mathbf{w}_E^H + \lambda_I \mathbf{w}_E^H \mathbf{h}_I^H \mathbf{h}_I - \lambda_E \mathbf{w}_E^H \mathbf{h}_E^H \mathbf{h}_E = \mathbf{0} \quad (8b)$$

$$\lambda_I \left(\mathbf{h}_I \mathbf{w}_E \mathbf{w}_E^H \mathbf{h}_I^H + \sigma^2 - \frac{1}{\gamma_0} \mathbf{h}_I \mathbf{w}_I \mathbf{w}_I^H \mathbf{h}_I^H \right) = 0 \quad (8c)$$

$$\lambda_E \left(\frac{E_0}{\eta} - \sigma^2 - \mathbf{h}_E \mathbf{w}_E \mathbf{w}_E^H \mathbf{h}_E^H - \mathbf{h}_E \mathbf{w}_I \mathbf{w}_I^H \mathbf{h}_E^H \right) = 0 \quad (8d)$$

Dependent on whether the SINR and energy constraint are active or not, in the following we discuss the optimality condition of the optimization problem and obtain the optimal beamforming vectors and the optimal transmit power P_{TX} .

1) *Only SINR Constraint is Active:* When only the SINR constraint is strictly met, this indicates that the SINR target is high and more demanding compared to the harvested energy requirement, which leads to the following proposition.

Proposition 1: When only the SINR constraint is active, the optimal beamforming vectors are given by

$$\mathbf{w}_I^* = \frac{\sqrt{\gamma_0 \sigma^2}}{(\mathbf{h}_I \mathbf{h}_I^H)} \cdot \mathbf{h}_I^H, \quad \mathbf{w}_E^* = \mathbf{0}, \quad (9)$$

the energy target E_0 of the EH receiver should satisfy

$$E_0 \leq \frac{\gamma_0 \eta \sigma^2 (\mathbf{h}_I \mathbf{h}_E^H \mathbf{h}_E \mathbf{h}_I^H)}{(\mathbf{h}_I \mathbf{h}_I^H)^2} + \eta \sigma^2, \quad (10)$$

and the optimal transmit power is

$$P_{TX}^* = \frac{\gamma_0 \sigma^2}{(\mathbf{h}_I \mathbf{h}_I^H)}. \quad (11)$$

Proof: See Appendix A.

2) *Only Energy Constraint is Active:* When only the energy constraint is active, this indicates that the harvested energy requirement is more demanding, which leads to the following proposition.

Proposition 2: When only the energy constraint is active, the optimal beamforming vectors are given by

$$\mathbf{w}_I^* = \frac{\sqrt{\frac{E_0 - \eta \sigma^2}{\eta(1+c^2)}}}{(\mathbf{h}_E \mathbf{h}_E^H)} \cdot \mathbf{h}_E^H, \quad \mathbf{w}_E^* = c \cdot \mathbf{w}_I^*, \quad (12)$$

where $c \geq 0$ and satisfies (73) which is shown in Appendix B. The harvested energy requirement E_0 should satisfy

$$E_0 \geq \frac{\gamma_0 \eta \sigma^2 (\mathbf{h}_E \mathbf{h}_E^H)^2}{(\mathbf{h}_I \mathbf{h}_E^H \mathbf{h}_E \mathbf{h}_I^H)} + \eta \sigma^2, \quad (13)$$

and the obtained optimal transmit power is

$$P_{TX}^* = \frac{E_0 - \eta \sigma^2}{\eta (\mathbf{h}_E \mathbf{h}_E^H)}. \quad (14)$$

Proof: See Appendix B.

We observe in (14) that the required transmit power is independent of c . This can be inferred from the optimization problem, as the EH receiver harvests the energy from both the information beamformer and the energy beamformer. As long as the value of c satisfies (73) (this guarantees that the SINR target of the ID is met), how the power is distributed between \mathbf{w}_I and \mathbf{w}_E according to (71) will not have an impact on the total amount of energy harvested by the EH receiver. We note that by choosing $c = 0$, the optimality is equivalent to employing the information beamformer only.

we note that if $\lambda_E = 0$, the optimal solution will be the same as (9), which corresponds to the extreme point before which the energy constraint is not active and the optimal solution is to employ information beamformer only. If $\lambda_E = 0$, the optimal solution will be (12). Therefore in this section,

3) *Both Constraints are Active:* When both the SINR constraint and energy constraint are active, we focus on the case where $\lambda_I > 0$ and $\lambda_E > 0$, as in this case $\lambda_E = 0$ leads to (9) and $\lambda_I = 0$ leads to (12). Subsequently, in the case of $\lambda_I > 0$ and $\lambda_E > 0$, the following proposition is obtained.

Proposition 3: When both the SINR constraint and energy constraint are active, the optimal beamforming vectors can be expressed as

$$\mathbf{w}_I^* = \alpha \cdot \mathbf{h}_I^H + \beta \cdot \mathbf{h}_\perp^H, \quad \mathbf{w}_E^* = \mathbf{0}, \quad (15)$$

where $\mathbf{h}_\perp = \mathbf{h}_E - \frac{\mathbf{h}_E \mathbf{h}_I^H \mathbf{h}_I}{(\mathbf{h}_I \mathbf{h}_I^H)}$, and α, β are the weighting factors. The energy requirement for the EH receiver should satisfy

$$\frac{\gamma_0 \eta \sigma^2 (\mathbf{h}_I \mathbf{h}_E^H \mathbf{h}_E \mathbf{h}_I^H)}{(\mathbf{h}_I \mathbf{h}_I^H)^2} + \eta \sigma^2 < E_0 < \frac{\gamma_0 \eta \sigma^2 (\mathbf{h}_E \mathbf{h}_E^H)^2}{(\mathbf{h}_I \mathbf{h}_E^H \mathbf{h}_E \mathbf{h}_I^H)} + \eta \sigma^2, \quad (16)$$

and the corresponding transmit power required is

$$P_{TX}^* = \lambda_I \sigma^2 + \lambda_E \left(\frac{E_0}{\eta} - \sigma^2 \right). \quad (17)$$

Proof: See Appendix C.

Condition of E_0	\mathbf{w}_I^*	\mathbf{w}_E^*	P_{TX}^*
$E_0 \leq \frac{\gamma_0 \eta \sigma^2 (\mathbf{h}_I \mathbf{h}_E^H \mathbf{h}_E \mathbf{h}_I^H)}{(\mathbf{h}_I \mathbf{h}_I^H)^2} + \eta \sigma^2$	$\frac{\sqrt{\gamma_0 \sigma^2}}{(\mathbf{h}_I \mathbf{h}_I^H)} \cdot \mathbf{h}_I^H$	$\mathbf{0}$	$\frac{\gamma_0 \sigma^2}{(\mathbf{h}_I \mathbf{h}_I^H)}$
$\frac{\gamma_0 \eta \sigma^2 (\mathbf{h}_I \mathbf{h}_E^H \mathbf{h}_E \mathbf{h}_I^H)}{(\mathbf{h}_I \mathbf{h}_I^H)^2} + \eta \sigma^2 < E_0 < \frac{\gamma_0 \eta \sigma^2 (\mathbf{h}_E \mathbf{h}_E^H)}{(\mathbf{h}_I \mathbf{h}_E^H \mathbf{h}_E \mathbf{h}_I^H)} + \eta \sigma^2$	$\alpha \cdot \mathbf{h}_I^H + \beta \cdot \mathbf{h}_\perp^H$	$\mathbf{0}$	$\lambda_I \sigma^2 + \lambda_E \left(\frac{E_0}{\eta} - \sigma^2 \right)$
$E_0 \geq \frac{\gamma_0 \eta \sigma^2 (\mathbf{h}_E \mathbf{h}_E^H)}{(\mathbf{h}_I \mathbf{h}_E^H \mathbf{h}_E \mathbf{h}_I^H)} + \eta \sigma^2$	$\frac{\sqrt{\frac{E_0 - \eta \sigma^2}{\eta(1+c^2)}}}{(\mathbf{h}_E \mathbf{h}_E^H)} \cdot \mathbf{h}_E^H$	$c \cdot \mathbf{w}_I^*$	$\frac{E_0 - \eta \sigma^2}{\eta (\mathbf{h}_E \mathbf{h}_E^H)}$

TABLE I: Optimal beamformers and the corresponding transmit power required for the case of one ID and one EH Receiver

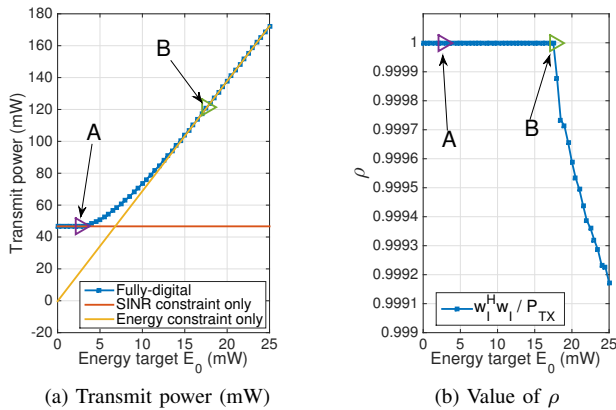


Fig. 2: $N_t = 12$, one ID, $K = 1$ EH receiver, $\gamma_0 = 16$ dB

We then summarize the optimal information beamformer, energy beamformer and the required transmit power for the case of one ID and one EH receiver in Table I.

To validate our above analyses, in Fig. 2 (a) and Fig. 2 (b) we depict the transmit power and the power ratio ρ with respect to the harvested energy requirement E_0 respectively, where ρ represents the percentage that the information beamformer accounts for the total transmit power, defined as

$$\rho = \frac{\mathbf{w}_I^H \mathbf{w}_I}{P_{TX}}. \quad (18)$$

In Fig. 2, the point 'A' denotes the extreme point before which the harvested energy constraint is not active, and $E_0^A = E_{th}^1$. The point 'B' is the extreme point after which the energy beamformer can be introduced, and $E_0^B = E_{th}^2$. When $E_0 \leq E_{th}^1$, there is only information beamformer and only the SINR constraint is active, in which case the required transmit power remains constant; When $E_{th}^1 < E_0 < E_{th}^2$, both of the constraints are active; When $E_0 \geq E_{th}^2$, the energy beamformer can be introduced, as validated in Fig. 2 (b), and the required transmit power is linearly increasing with the increasing harvested energy requirement E_0 , as given by (79).

B. The Case of K EH Receivers

For a more general case of $K > 1$ EH receivers in the system, the optimal solution is not unique and it is generally difficult to derive the closed-form solutions of the optimization

problem, and we only discuss the optimality condition of the problem, which is detailed in the following.

1) *Only SINR Constraint is Active:* This case is similar to the case where there is only one EH receiver, and the optimal beamforming scheme will be to employ the information beamformer only, which is obtained in (9). The harvested energy requirement should satisfy

$$E_0 \leq \min_k \left[\eta \mathbf{h}_E^k \mathbf{w}_I \mathbf{w}_I^H (\mathbf{h}_E^k)^H + \eta \sigma^2 \right] \\ \Rightarrow E_0 \leq \min_k \left\{ \frac{\gamma_0 \eta \sigma^2 \left[\mathbf{h}_I (\mathbf{h}_E^k)^H \mathbf{h}_E^k \mathbf{h}_I^H \right]}{(\mathbf{h}_I \mathbf{h}_I^H)^2} + \eta \sigma^2 \right\}. \quad (19)$$

2) *Only Harvested Energy Constraints are Active:* This corresponds to the case where the harvested energy requirement is high, and we can obtain $\lambda_I = 0$ since the SINR constraint is not active. Subsequently, it is easy to observe from the stationarity conditions that each \mathbf{w}_E^i is parallel to \mathbf{w}_I , and therefore we can express each \mathbf{w}_E^i as

$$\mathbf{w}_E^i = c_i \cdot \mathbf{w}_I, \quad \forall i \in \mathcal{K}. \quad (20)$$

With the SINR constraint being over-satisfied, we can further obtain $\sum_{i=1}^K c_i^2 < \frac{1}{\gamma_0}$ by following a similar approach in (73). Accordingly, the power ratio ρ defined in (18) for the case of $K > 1$ EH receivers can be further obtained as

$$\rho = \frac{\mathbf{w}_I^H \mathbf{w}_I}{\mathbf{w}_I^H \mathbf{w}_I + \sum_{i=1}^K c_i^2 \mathbf{w}_I^H \mathbf{w}_I} = \frac{1}{1 + \sum_{i=1}^K c_i^2} \\ \Rightarrow \rho > \frac{1}{1 + \frac{1}{\gamma_0}} = \frac{\gamma_0}{1 + \gamma_0}.$$

Note that by setting each $c_i = 0$, $\forall i \in \mathcal{K}$, we obtain $\rho = 1$, which means that the optimality can still be achieved by employing the information beamformer only.

3) *Both Constraints are Active:* In this case, based on the derivation in (77)-(79), we can similarly obtain the total transmit power as

$$P_{TX} = \lambda_I \sigma^2 + \sum_{k=1}^K \lambda_E^k \left(\frac{E_0}{\eta} - \sigma^2 \right). \quad (22)$$

By following a similar approach in Appendix C, it is shown by contradiction that the optimality is achieved by employing only the information beamformer, and $(\mathbf{w}_E^i)^* = \mathbf{0}$, $\forall i \in \mathcal{K}$.

To summarize, for both the special case of one EH receiver and the case of multiple EH receivers, the optimal transmit power can be obtained by employing the information beamformer \mathbf{w}_I only. This can also be observed based on the fact that EH receivers do not need to decode the symbols, and therefore energy beamforming is indeed not necessary. Our contribution here is that we mathematically prove the above observation and obtain the closed-form expressions for the special case of $K = 1$ EH receiver with the above analysis.

C. Semi-Definite Relaxation (SDR) Approach to Solve \mathcal{P}_1

By introducing $\mathbf{W}_I = \mathbf{w}_I \mathbf{w}_I^H$, $\mathbf{D}_I = \mathbf{h}_I^H \mathbf{h}_I$ and $\mathbf{D}_E^k = (\mathbf{h}_E^k)^H \mathbf{h}_E^k$, \mathcal{P}_1 can be simplified and further transformed into a semi-definite programming (SDP), given by

$$\begin{aligned} \mathcal{P}_3: \quad & \min_{\mathbf{W}_I} \text{tr} \{ \mathbf{W}_I \} \\ \text{s.t.} \quad & \frac{1}{\gamma_0} \text{tr} \{ \mathbf{D}_I \mathbf{W}_I \} \geq \sigma^2 \\ & \text{tr} \{ \mathbf{D}_E^k \mathbf{W}_I \} + \sigma^2 \geq \frac{E_0}{\eta}, \forall k \in \mathcal{K} \\ & \mathbf{W}_I \succeq 0, \text{rank} \{ \mathbf{W}_I \} = 1 \end{aligned} \quad (23)$$

By dropping the rank-1 constraint for \mathbf{W}_I in \mathcal{P}_3 , the relaxed optimization problem becomes convex, and can be efficiently solved by convex optimization tools such as CVX. When $\text{rank} \{ \mathbf{W}_I^* \} = 1$, the solution to \mathcal{P}_1 can be obtained by employing the eigenvalue decomposition of \mathbf{W}_I^* , given by

$$\mathbf{w}_I^* = \mathbf{U} \Sigma^{1/2}, \quad (24)$$

where \mathbf{U} and Σ correspond to the eigenvectors and eigenvalues of \mathbf{W}_I^* respectively, and we have $\mathbf{W}_I^* = \mathbf{U} \Sigma \mathbf{U}^H$. It has been shown in [44][45] that the solution for the relaxed version of \mathcal{P}_3 satisfies

$$\text{rank} (\mathbf{W}_I^*) \leq \sqrt{K+1}. \quad (25)$$

Therefore, when there are no more than 2 EH receivers in the system ($K \leq 2$), explicitly we have $\sqrt{K+1} < 2$ and the obtained solution is guaranteed to be rank-1, which means that in this case SDR is not a relaxation but an optimal solution to the original problem. When $K > 2$, while the obtained solution cannot be guaranteed to be rank-1, we show below in Table II that in most cases the obtained solutions still satisfy the rank-1 constraint and are therefore optimal when the number of EH receivers K is small. The results in Table II are obtained based on 5000 channel realizations with $N_t = 12$, $\eta = 0.35$, $E_0 = 5\text{mW}$ and $\gamma_0 = 10\text{dB}$. When the obtained rank of \mathbf{W}_I^* is larger than 1, we can obtain a feasible close-to-optimal solution as

$$\mathbf{w}_I = \tau \cdot \mathbf{w}_I^* = \tau \cdot \mathbf{U} \Sigma^{1/2}, \quad (26)$$

where $\tau \geq 1$ and can be obtained as

$$\tau = \max \left\{ \sqrt{\frac{\gamma_I \sigma^2}{|\mathbf{h}_I \mathbf{U} \Sigma^{1/2}|^2}}, \sqrt{\frac{E_1 - \eta \sigma^2}{\eta |\mathbf{h}_E^1 \mathbf{U} \Sigma^{1/2}|^2}}, \dots, \sqrt{\frac{E_K - \eta \sigma^2}{\eta |\mathbf{h}_E^K \mathbf{U} \Sigma^{1/2}|^2}} \right\}, \quad (27)$$

which guarantees that all the constraints in \mathcal{P}_1 are met. Therefore, for the small-scale system considered in this paper,

Number of Users ($1 + K$)	1	2	3	4	5
Average rank of \mathbf{W}_I^*	1	1	1	1.0528	1.1736
Maximum rank of \mathbf{W}_I^*	1	1	1	2	2
Rank-1 percentage of \mathbf{W}_I^*	100%	100%	100%	94.72%	82.64%

TABLE II: Average rank, maximum rank and rank-1 percentage of \mathbf{W}_I^* for \mathcal{P}_3 , $N_t = 12$, $\eta = 0.35$, $E_0 = 5\text{mW}$, $\gamma_0 = 10\text{dB}$

the SDR approach can be effectively applied to obtain the solution of \mathcal{P}_1 and the optimization problems in the following sections.

IV. A LOW-COMPLEXITY HYBRID BEAMFORMING SCHEME BASED ON SVD

The fully-digital MIMO SWIPT system discussed in Section III requires a dedicated RF chain for each antenna element, which is inefficient in both the hardware complexity and power consumption. Towards energy-efficient SWIPT, we proceed to study the hybrid structure, and we firstly consider a low-complexity hybrid beamforming for SWIPT in this section as a performance benchmark, where the BS employs N_{RF}^t ($1 \leq N_{RF}^t < N_t$) RF chains and the beamforming is divided into the analog domain and the digital domain. Then, we can express the transmit signal vector as

$$\mathbf{x} = \mathbf{F}_{RF} \mathbf{F}_{BB} \mathbf{s}, \quad (28)$$

where $\mathbf{s} = [s_I, s_E^1, s_E^2, \dots, s_E^K]^T$ is the data symbol vector, and $\mathbf{s} \in \mathcal{C}^{(K+1) \times 1}$. $\mathbf{F}_{BB} \in \mathcal{C}^{N_{RF}^t \times (K+1)}$ represents the digital beamformer and can be decomposed as

$$\mathbf{F}_{BB} = [\mathbf{f}_I, \mathbf{f}_E^1, \mathbf{f}_E^2, \dots, \mathbf{f}_E^K]. \quad (29)$$

$\mathbf{F}_{RF} \in \mathcal{C}^{N_t \times N_{RF}^t}$ denotes the analog beamformer implemented with phase shifters. When a fully-connected structure is considered, as shown in Fig. 3 (a), each entry of \mathbf{F}_{RF} satisfies the constant modulus constraint, which can be expressed as

$$[\mathbf{F}_{RF}]_{m,n} = e^{j\varphi_{m,n}}. \quad (30)$$

For partially-connected structures, as shown in Fig. 3 (b), \mathbf{F}_{RF} becomes a block-diagonal matrix and can be expressed as

$$\mathbf{F}_{RF} = \begin{bmatrix} \mathbf{f}_1^p & & & \\ & \mathbf{f}_2^p & & \\ & & \ddots & \\ & & & \mathbf{f}_{N_{RF}^t}^p \end{bmatrix}, \quad (31)$$

where each $\mathbf{f}_k^p \in \mathcal{C}^{M \times 1}$ and $M = N_t / N_{RF}^t$ denotes the number of antennas connected to each RF chain. In this case, each entry of \mathbf{f}_k^p satisfies

$$[\mathbf{f}_k^p]_m = e^{j\phi_{m,k}}. \quad (32)$$

In this section, a low-complexity hybrid beamforming scheme for MIMO SWIPT is proposed based on SVD, which serves as a benchmark to be compared with the proposed iterative scheme in Section V. When the hybrid beamforming scheme is applied, it is generally difficult to directly solve

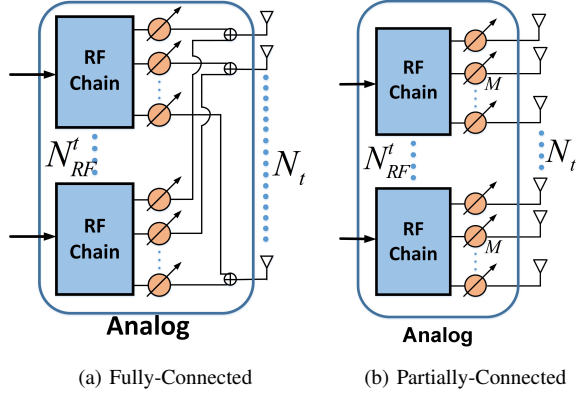


Fig. 3: Transmit array structures

the joint optimization problem due to the non-convex constant modulus constraint of the analog beamformer, which is in the form of (30). Therefore, to remove the non-convex constant modulus constraint in the optimization problem, it is intuitive that we firstly design the analog beamformer \mathbf{F}_{RF} , followed by the design of the low-dimensional digital beamformer \mathbf{F}_{BB} with convex optimization. To be specific, we firstly express the SVD of the channel as

$$\mathbf{H} = \mathbf{U}\mathbf{\Sigma}\mathbf{V}^H, \quad (33)$$

where \mathbf{U} and $\mathbf{V} = [\mathbf{v}_1, \mathbf{v}_2, \dots, \mathbf{v}_{N_t}]$ are the left- and right-singular vectors. Then, each phase $\varphi_{m,n}$ of the analog beamformer \mathbf{F}_{RF} is selected as

$$\varphi_{m,n} = \theta_{m,n}, \quad m \in \mathcal{M}, \quad n \in \mathcal{N}, \quad (34)$$

where $\mathcal{N} = \{1, 2, \dots, N_{RF}^t\}$ and $\theta_{m,n}$ is the phase of the m -th element in \mathbf{v}_n . While we employ an analog beamforming design based on SVD, other channel-dependent analog designs can also be applied. With \mathbf{F}_{RF} obtained, the optimization problem to obtain \mathbf{F}_{BB} can be formulated as

$$\begin{aligned} \mathcal{P}_4 : \quad & \min_{\mathbf{f}_I, \mathbf{f}_E^i} \|\mathbf{F}_{RF}\mathbf{f}_I\|^2 + \sum_{i=1}^K \|\mathbf{F}_{RF}\mathbf{f}_E^i\|^2 \\ \text{s.t.} \quad & \gamma_I \geq \gamma_0 \\ & E_k \geq E_0, \quad \forall k \in \mathcal{K} \end{aligned} \quad (35)$$

While the analysis in Section III is conducted only for the fully-digital beamforming schemes, similar analysis can be performed for \mathcal{P}_4 of the hybrid beamforming, since in such case the analog beamformer \mathbf{F}_{RF} can be regarded as a fixed matrix. A similar conclusion can be drawn that the optimality for \mathcal{P}_4 is to employ the low-dimensional information beamformer only, and therefore the SDP form of \mathcal{P}_4 can be simplified into

$$\begin{aligned} \mathcal{P}_5 : \quad & \min_{\mathbf{F}_I} \text{tr} \{ \mathbf{F}_{RF}\mathbf{F}_I\mathbf{F}_{RF}^H \} \\ \text{s.t.} \quad & \text{tr} \{ \mathbf{D}_I\mathbf{F}_{RF}\mathbf{F}_I\mathbf{F}_{RF}^H \} \geq \gamma_0\sigma^2 \\ & \text{tr} \{ \mathbf{D}_E^k\mathbf{F}_{RF}\mathbf{F}_I\mathbf{F}_{RF}^H \} \geq \frac{E_0}{\eta} - \sigma^2, \quad \forall k \in \mathcal{K} \\ & \mathbf{F}_I \succeq 0, \quad \text{rank} \{ \mathbf{F}_I \} = 1 \end{aligned} \quad (36)$$

where $\mathbf{F}_I = \mathbf{f}_I\mathbf{f}_I^H$. By dropping the rank-1 constraint, \mathcal{P}_5 can also be effectively solved. As the rank of the obtained \mathbf{F}_I is only related to the number of users ($1 + K$), the rank result and approach in Section III-C can be trivially extended to the hybrid case of \mathcal{P}_5 .

A. Extension to Partially-Connected Structures

When partially-connected structures are considered, the analog beamformer \mathbf{F}_{RF} becomes block-diagonal as shown in (31), where each $\mathbf{f}_k^p \in \mathcal{C}^{M \times 1}$. Similar to the design for the fully-connected structures, each entry of \mathbf{f}_k^p for the partially-connected structures can be obtained as

$$[\mathbf{f}_k^p]_m = e^{j\theta_{n,k}}, \quad (37)$$

where $\theta_{n,k}$ denotes the phase of the k -th entry in \mathbf{v}_n , and we have $k = (n-1)M + m$. As can be seen, the analog beamformer for the partially-connected structures can only exploit part of the channel, which will lead to an increased transmit power P_{TX} to achieve the same performance requirements compared to the fully-connected structures. We further note however, that due to the reduced number of RF chains and phase shifters required, the total power consumption P_{BS} for partially-connected structures will in fact be much lower than the fully-digital case and fully-connected structures. We shall quantify this tradeoff in terms of the total power consumption at the BS in Section VII.

V. ITERATIVE HYBRID BEAMFORMING BASED ON A GEOMETRICAL APPROACH

Based on the results given in Table I and the analysis in Section III, it is observed that the optimal beamforming scheme is to employ the information beamformer \mathbf{w}_I only (by noting that each c_i can be set to 0), and the resulting beamforming matrix for the fully-digital case is therefore obtained as

$$\mathbf{W} = [\mathbf{w}_I, \mathbf{0}^{N_t \times K}]. \quad (38)$$

Similarly, by considering the effective channel expression, the optimal low-dimensional digital beamformer for the hybrid scheme in the optimization problem \mathcal{P}_4 will be

$$\mathbf{F}_{BB} = [\mathbf{f}_I, \mathbf{0}^{(K+1) \times K}]. \quad (39)$$

Then, based on these two observations, we propose an iterative scheme where we alternately update the analog beamformer and the digital beamformer. To be specific, for the design of the analog beamformer \mathbf{F}_{RF} , instead of employing the SVD, we propose to minimize the difference between the optimal fully-digital beamformer and the hybrid beamformer, which can be formulated as

$$\begin{aligned} \mathcal{P}_6 : \quad & \min_{\mathbf{F}_{RF}} \|\mathbf{W} - \mathbf{F}_{RF}\mathbf{F}_{BB}\|^2 \\ \text{s.t.} \quad & \mathbf{F}_{RF} \in \mathcal{F} \end{aligned} \quad (40)$$

where we denote \mathcal{F} as the set that consists of the matrices that satisfy the constant modulus constraint for each of their entries. Based on the analysis in Section III that the optimality

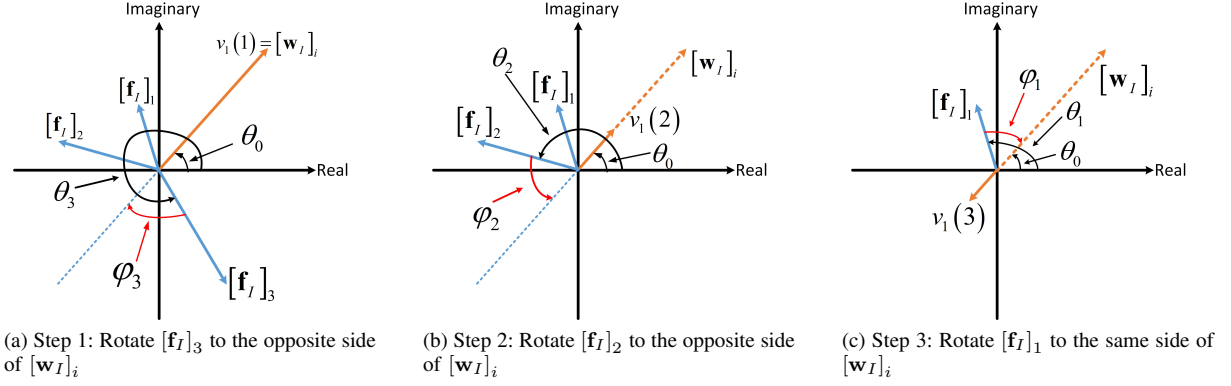


Fig. 4: Geometric interpretation of \mathcal{P}_8^i and the solution for the example of one ID and $K = 2$ EH receivers

can be achieved by the information beamformer only, the objective function of \mathcal{P}_6 can be further decomposed as

$$\begin{aligned} & \|\mathbf{W} - \mathbf{F}_{RF}\mathbf{F}_{BB}\|^2 \\ &= \left\| [\mathbf{w}_I, \mathbf{0}^{N_t \times K}] - \mathbf{F}_{RF} [\mathbf{f}_I, \mathbf{0}^{(K+1) \times K}] \right\|^2 \\ &= \|\mathbf{w}_I - \mathbf{F}_{RF}\mathbf{f}_I\|^2 \\ &= \sum_{i=1}^{N_t} \left\| [\mathbf{w}_I]_i - \mathbf{f}_{RF}^i \mathbf{f}_I \right\|^2, \end{aligned} \quad (41)$$

where we note that each $[\mathbf{w}_I]_i$ is a scalar. $\mathbf{f}_{RF}^i \in \mathcal{C}^{1 \times (K+1)}$ is the i -th row of \mathbf{F}_{RF} and we decompose $\mathbf{F}_{RF} = \left[(\mathbf{f}_{RF}^1)^T, (\mathbf{f}_{RF}^2)^T, \dots, (\mathbf{f}_{RF}^{N_t})^T \right]^T$. As can be observed in (41), the objective function is decomposed into N_t independent sub-functions by row, and therefore the optimization problem \mathcal{P}_6 is equivalent to minimizing each of the N_t independent sub-problems. We formulate the i -th sub-problem as

$$\begin{aligned} \mathcal{P}_7^i: & \min_{\mathbf{f}_{RF}^i} \left| [\mathbf{w}_I]_i - \mathbf{f}_{RF}^i \mathbf{f}_I \right| \\ \text{s.t.} & \mathbf{f}_{RF}^i \in \mathcal{G} \end{aligned} \quad (42)$$

where \mathcal{G} denotes the set of row vectors that satisfy the constant modulus constraint for each of their entries. For simplicity we introduce

$$[\mathbf{t}]_m = [\mathbf{f}_{RF}^i]_m [\mathbf{f}_I]_m. \quad (43)$$

Then, the optimization problem can be further transformed into

$$\begin{aligned} \mathcal{P}_8^i: & \min_{\mathbf{f}_{RF}^i} |u_i| \\ \text{s.t.} & u_i = [\mathbf{w}_I]_i - \sum_{m=1}^{K+1} [\mathbf{t}]_m \\ & \mathbf{f}_{RF}^i \in \mathcal{G} \end{aligned} \quad (44)$$

A. Optimal Analog Beamformer Solution via a Geometrical Representation

As each entry of \mathbf{f}_{RF}^i is of constant modulus, therefore the multiplication of each $[\mathbf{f}_{RF}^i]_m$ to the corresponding $[\mathbf{f}_I]_m$ in (43) can be regarded as the effect of an angle rotation in the complex plane. Moreover, since $[\mathbf{w}_I]_i$ in \mathcal{P}_8^i is a scalar, we can therefore employ a geometric representation to arrive

at an optimal solution efficiently. An explanatory geometrical representation for the case of one ID and $K = 2$ EH receivers is shown in Fig. 4, where the dashed brown arrow represents the optimal fully-digital solution $[\mathbf{w}_I]_i$, the solid brown arrow denotes $v_i(m)$ that is to be introduced in (46), and the solid blue arrows denote each entry in \mathbf{f}_I . We denote θ_0 as the phase of $[\mathbf{w}_I]_i$, θ_m as the phase of $[\mathbf{f}_I]_m$, and we assume $\theta_0, \theta_m \in [0, 2\pi)$, as shown in Fig. 4, where it can be observed geometrically that the optimal solution for \mathbf{f}_{RF}^i that minimizes $|u_i|$ in \mathcal{P}_8^i is to rotate each $[\mathbf{f}_I]_m$ such that each resulting $[\mathbf{t}]_m$ is collinear to $[\mathbf{w}_I]_i$. Then, we introduce the algorithm employed to solve the sub-problem \mathcal{P}_8^i based on successive phase rotation. To be specific, to achieve collinearity for each resulting $[\mathbf{t}]_m$, the phase of the corresponding $[\mathbf{f}_{RF}^i]_m$ can be obtained based on Fig. 4 as

$$\varphi_m = \theta_0 - \theta_m, \text{ or } \varphi_m = \theta_0 + \pi - \theta_m, \quad (45)$$

which is dependent on whether $[\mathbf{f}_I]_m$ is rotated to the same direction of $[\mathbf{w}_I]_i$ or the opposite direction of $[\mathbf{w}_I]_i$. Define a function v_i with respect to m that represents the difference between the optimal fully-digital beamformer and the sum of the previously rotated components of \mathbf{f}_I as

$$v_i(m) = [\mathbf{w}_I]_i - \sum_{j=1}^{m-1} [\mathbf{t}]_j, \quad (46)$$

and we further define $v_i(1) = [\mathbf{w}_I]_i$. $v_i(m)$ therefore represents the residual portion of $[\mathbf{w}_I]_i$ to be cancelled. It is then observed that the value of each φ_m is dependent on the residual portion $v_i(m)$. Moreover, to guarantee optimum and that the resulting objective function $|u_i|$ in \mathcal{P}_8^i is minimized, one should sort the elements in \mathbf{f}_I in the descending order of amplitude, and the elements with larger amplitudes should be rotated first. For example, in Fig. 4, $[\mathbf{f}_I]_3$ has the largest amplitude compared to $[\mathbf{f}_I]_1$ and $[\mathbf{f}_I]_2$, and therefore we firstly rotate $[\mathbf{f}_I]_3$ to the opposite side of $[\mathbf{w}_I]_i$ and $\varphi_3 = \theta_0 + \pi - \theta_3$, which is shown in Fig. 4 (a) and leads to Fig. 4 (b); Then, in Fig. 4 (b), since $[\mathbf{f}_I]_2$ has a larger amplitude compared to $[\mathbf{f}_I]_1$ and the phase of $v_i(2)$ is the same as that of $[\mathbf{w}_I]_i$, therefore $[\mathbf{f}_I]_2$ is rotated to the opposite side of $[\mathbf{w}_I]_i$ and $\varphi_2 = \theta_0 + \pi - \theta_2$, which leads to Fig. 4 (c); In Fig. 4 (c), since the phase of $v_i(3)$ is the opposite of $[\mathbf{w}_I]_i$, then $[\mathbf{f}_I]_1$ is rotated to the same direction of $[\mathbf{w}_I]_i$, and $\varphi_1 = \theta_0 - \theta_1$.

In fact, for each $[\mathbf{f}_{RF}^i]_m$, it should be rotated to the opposite side of $v_i(m)$, which can also be observed from the definition of $v_i(m)$. We then summarize the above algorithm to obtain \mathbf{f}_{RF}^i in Algorithm 1.

Algorithm 1 Optimal Analog Beamformer Solution for \mathcal{P}_8^i

input : $[\mathbf{w}_I]_i, \mathbf{f}_I$; **output** : \mathbf{f}_{RF}^i .
 $\theta_0 = \arg \{[\mathbf{w}_I]_i\}, \hat{\mathbf{f}}_I = \text{sort}(\mathbf{f}_I, d)$.
for $m = 1 : N_{RF}^i$ **do**
 $m_0 = \text{find} \left\{ \left[\hat{\mathbf{f}}_I \right]_m = \mathbf{f}_I \right\}$, then $\theta_{m_0} = \arg \{[\mathbf{f}_I]_{m_0}\}$;
 Calculate $v_i(m)$.
if $\arg \{v_i(m)\} = \arg \{[\mathbf{w}_I]_i\}$ **then**
 $\varphi_{m_0} = \theta_0 + \pi - \theta_{m_0}$.
end if
if $\arg \{v_i(m)\} = \pi + \arg \{[\mathbf{w}_I]_i\}$ **then**
 $\varphi_{m_0} = \theta_0 - \theta_{m_0}$.
end if
 $[\mathbf{f}_{RF}^i]_{m_0} = e^{j\varphi_{m_0}}$.
end for

In Algorithm 1, $\hat{\mathbf{a}} = \text{sort}(\mathbf{a}, d)$ denotes the function that sorts the elements of \mathbf{a} in a descending order of amplitude, and the re-ordered vector is denoted as $\hat{\mathbf{a}}$. The function $x = \text{find} \{a = \mathbf{b}\}$ means that $[\mathbf{b}]_x = a$, and we denote $\arg \{a\}$ as the phase of a . With the above algorithm, the optimal \mathbf{f}_{RF}^i can be efficiently obtained and the resulting $|u_i|$ is guaranteed to be the minimal. We perform Algorithm 1 to calculate each \mathbf{f}_{RF}^i for N_t times, and then the optimal analog beamformer \mathbf{F}_{RF} can be obtained.

B. Iterative Design

It is observed that the above design of each \mathbf{f}_{RF}^i requires the knowledge of the digital beamformer \mathbf{f}_I , we then propose an iterative design where we alternately update \mathbf{F}_{RF} and \mathbf{F}_{BB} until convergence or a maximum number of iterations is reached. The proposed algorithm is then summarized in Algorithm 2, where \mathbf{w}_I is the optimal fully-digital beamformer for \mathcal{P}_3 in Section III, \mathbf{F}_{BB}^0 is the initial low-dimensional digital beamformer of the hybrid scheme obtained from \mathcal{P}_5 in Section IV, and N_{max} denotes the maximum iteration number. We introduce Δ as a variable that represents the convergence accuracy, and Δ_{th} denotes the accuracy threshold.

Algorithm 2 The Iterative Hybrid Beamforming Design

input : $\mathbf{w}_I, \mathbf{F}_{BB}^0$. **output** : $\mathbf{F}_{RF}^*, \mathbf{F}_{BB}^*$.
 $n = 0, \mathbf{W}_h^{(0)} = \mathbf{0}$.
while $n \leq N_{max}$ and $\Delta \geq \Delta_{th}$ **do**
 Obtain $\mathbf{f}_I^{(n)}$ from $\mathbf{F}_{BB}^{(n)}$ based on (51)
 Obtain $\mathbf{F}_{RF}^{(n+1)}$ by Algorithm 1 with $\mathbf{f}_I^{(n)}$
 Obtain $\mathbf{F}_{BB}^{(n+1)}$ by solving \mathcal{P}_5 with $\mathbf{F}_{RF}^{(n+1)}$
 $\mathbf{W}_h^{(n+1)} = \mathbf{F}_{RF}^{(n+1)} \mathbf{F}_{BB}^{(n+1)}, \Delta = \left\| \mathbf{W}_h^{(n+1)} - \mathbf{W}_h^{(n)} \right\|$
 $n = n + 1$
end while
 $\mathbf{F}_{RF}^* = \mathbf{F}_{RF}^{(n)}, \mathbf{F}_{BB}^* = \mathbf{F}_{BB}^{(n)}$.

Convergence: It has been shown in Table II that for the considered small-scale system, in most cases the SDR approach can obtain the optimal rank-1 solution. In this case, since the sub-problems to obtain \mathbf{F}_{RF} and \mathbf{F}_{BB} in each iteration are solved optimally, the iterative design in Algorithm 2 is guaranteed to converge [46][47]. Nevertheless, when the rank of the obtained solution is larger than 1, while the convergence cannot be explicitly proven, a feasible close-to-optimal solution can be obtained based on (26)-(27), and it is observed in our simulations that the proposed scheme is also shown to be convergent. Furthermore, our scheme also includes a maximum number of iterations N_{max} to terminate the iterations and return a solution.

C. Computational Complexity Analysis

For both of the proposed schemes, it is observed that the dominant complexity arises from solving the optimization problems by CVX. For each optimization problem, CVX firstly transforms the original problem into the dual problem, which is then solved by the interior-point algorithms. Based on [22][48], the complexity of the interior-point algorithm for solving the dual problem of an M -dimensional optimization with N variables requires $\mathcal{O} \left\{ \sqrt{NM} (N^3 M^2 + N^2 M^3) \right\}$ operations. For the fully-digital scheme based on the optimization problem \mathcal{P}_3 , \mathbf{W}_I and each \mathbf{W}_E^i are N_t -dimensional, and there is one ID and K EH receivers in the system, which leads to $M = N_t$, and $N = K + 1$. For the proposed hybrid scheme based on SVD, we can similarly obtain that $M = K + 1$, and $N = K + 1$, and the complexity of the proposed iterative scheme will be N_{max} times higher than that of the hybrid scheme based on SVD, since CVX needs to be performed N_{max} times, as observed in Algorithm 2. We can then obtain the complexity of each scheme, which can be expressed as

$$\begin{aligned}
 C_{Fully} &= \mathcal{O} \left\{ \sqrt{(K+1)N_t} \left[(K+1)^3 N_t^2 + (K+1)^2 N_t^3 \right] \right\}, \\
 C_{Hybrid}^{PC} &= \mathcal{O} \left\{ \sqrt{(K+1)(K+1)} \left[2(K+1)^3 (K+1)^2 \right] \right\} \\
 &= \mathcal{O} \left\{ 2(K+1)^6 \right\}, \\
 C_{Hybrid}^{Iterative} &= \mathcal{O} \left\{ N_{max} (K+1) \left[2(K+1)^3 (K+1)^2 \right] \right\} \\
 &= \mathcal{O} \left\{ 2N_{max} (K+1)^6 \right\}.
 \end{aligned} \tag{47}$$

It is then observed that the complexity of both the hybrid schemes is irrelevant to the number of transmit antennas N_t at the BS, and the complexity-reduction gain will be higher when N_t increases. A representative MIMO SWIPT scenario is explored in Table III below, where the number of transmit antennas at the BS is $N_t = 12$, and the complexity of each scheme is compared with the increasing number of EH receivers.

It is also observed that compared to the fully-digital case, both of the proposed hybrid schemes require less computational complexity, and the hybrid scheme based on SVD is the most computationally efficient one.

Schemes	Number of UEs		
	1 ID, 3 EHs	1 ID, 4 EHs	1 ID, 5 EHs
Fully-digital	$\mathcal{O}(2.6 \times 10^5)$	$\mathcal{O}(4.7 \times 10^5)$	$\mathcal{O}(7.9 \times 10^5)$
Hybrid PC	$\mathcal{O}(8.1 \times 10^3)$	$\mathcal{O}(3.1 \times 10^4)$	$\mathcal{O}(9.3 \times 10^4)$
Hybrid Iterative	$\mathcal{O}(3.2 \times 10^4)$	$\mathcal{O}(1.2 \times 10^5)$	$\mathcal{O}(3.7 \times 10^5)$

TABLE III: Computational complexity of the fully-digital scheme and the hybrid schemes for $N_t = 12$, $N_{max} = 4$

D. Extension to Partially-Connected Structures

When partially-connected structures are considered for the proposed iterative design, each \mathbf{f}_{RF}^i in (42) only has one non-zero element, and we only need to rotate this entry to the opposite side of $[\mathbf{w}_I]_i$, which greatly simplifies the design. We then summarize the Algorithm to obtain \mathbf{F}_{RF} for partially-connected structures in Algorithm 3, where the function $\lceil x \rceil$ denotes the minimum integer that is not smaller than x .

Algorithm 3 Analog Beamformer of the Iterative Scheme for Partially-Connected Structures

input : $\mathbf{w}_I, \mathbf{f}_I$; **output** : \mathbf{F}_{RF} .
for $i = 1 : N_t$ **do**
 $\mathbf{f}_{RF}^i = \mathbf{0}^{1 \times (K+1)}$
 Obtain $[\mathbf{w}_I]_i$, then $\theta_0 = \arg \{[\mathbf{w}_I]_i\}$
 Calculate $m_0 = \lceil \frac{i}{M} \rceil$.
 $\theta_{m_0} = \arg \{[\mathbf{f}_I]_{m_0}\}$, $\phi_{m_0} = \theta_0 + \pi - \theta_{m_0}$
 $[\mathbf{f}_{RF}^i]_{m_0} = e^{j\phi_{m_0}}$.
end for
 $\mathbf{F}_{RF} = \left[(\mathbf{f}_{RF}^1)^T, (\mathbf{f}_{RF}^2)^T, \dots, (\mathbf{f}_{RF}^{N_t})^T \right]^T$.

VI. ROBUST HYBRID DESIGN FOR IMPERFECT CSI

In practical wireless communication scenarios, there exist errors in obtaining the CSI and the perfect CSI assumption is no longer valid. The channel estimation techniques for hybrid structures are still an ongoing topic, where some results and approaches can be found in [49]-[51]. To study the robust hybrid beamforming design for the proposed scheme, in this section we employ a generic additive CSI error model, given by [52]

$$\mathbf{h}_I = \hat{\mathbf{h}}_I + \mathbf{e}_I, \quad \mathbf{h}_E^k = \hat{\mathbf{h}}_E^k + \mathbf{e}_E^k, \quad \forall k \in \mathcal{K}. \quad (48)$$

The channel uncertainty is considered as bounded by a spherical region, which can be expressed as

$$\begin{aligned} \mathcal{D}_I &:= \left\{ \hat{\mathbf{h}}_I + \mathbf{e}_I \mid \|\mathbf{e}_I\| \leq \delta_0 \right\}, \\ \mathcal{D}_E^k &:= \left\{ \hat{\mathbf{h}}_E^k + \mathbf{e}_E^k \mid \|\mathbf{e}_E^k\| \leq \delta_0 \right\}, \quad \forall k \in \mathcal{K}, \end{aligned} \quad (49)$$

where δ_0 denotes the channel inaccuracy coefficient which defines the radius of the spherical region.

We then proceed to investigate the robust power minimization for imperfect CSI, where we propose to consider the channel uncertainty for the design of the digital beamformer while retaining the design of the analog beamformer as for perfect CSI in Section IV and V, where in the case of imperfect

CSI the analog beamformer is obtained based on $\hat{\mathbf{h}}_I$ and $\hat{\mathbf{h}}_E^k$. Then, the optimization problem to obtain the robust low-dimensional digital beamformers of the hybrid schemes can be formulated as

$$\begin{aligned} \mathcal{P}_9 : \quad & \min_{\hat{\mathbf{f}}_I} p \\ \text{s.t.} \quad & p \geq \left\| \hat{\mathbf{F}}_{RF} \hat{\mathbf{f}}_I \right\|^2 \\ & \left| \mathbf{h}_I \hat{\mathbf{F}}_{RF} \hat{\mathbf{f}}_I \right|^2 \geq \gamma_0 \sigma^2, \quad \forall \mathbf{h}_I \in \mathcal{D}_I \\ & \left| \mathbf{h}_E^k \hat{\mathbf{F}}_{RF} \hat{\mathbf{f}}_I \right|^2 \geq \frac{E_0}{\eta} - \sigma^2, \quad \forall k \in \mathcal{K}, \quad \forall \mathbf{h}_E^k \in \mathcal{D}_E^k \end{aligned} \quad (50)$$

where we note that the problem \mathcal{P}_9 contains infinite number of constraints and it is difficult to directly solve it. To guarantee that the constraints are met, we then consider the worst-case SINR for the ID, expressed as

$$\widetilde{\text{SINR}} = \min_{\mathbf{h}_I \in \mathcal{D}_I} \frac{\left| \mathbf{h}_I \hat{\mathbf{F}}_{RF} \hat{\mathbf{f}}_I \right|^2}{\sigma^2}. \quad (51)$$

Then, the SINR constraint in \mathcal{P}_9 is further transformed into

$$\widetilde{\text{SINR}} \geq \gamma_0, \quad \forall \mathbf{h}_I \in \mathcal{D}_I. \quad (52)$$

By defining a complex Hermitian matrix

$$\mathbf{U}_I = \frac{1}{\gamma_0} \hat{\mathbf{F}}_{RF} \hat{\mathbf{f}}_I \hat{\mathbf{f}}_I^H \hat{\mathbf{F}}_{RF}^H, \quad (53)$$

(52) is equivalent to: $\forall \mathbf{e}_I \mathbf{e}_I^H \leq \delta_0^2$,

$$\begin{aligned} & \mathbf{h}_I \mathbf{U}_I \mathbf{h}_I^H - \sigma^2 \geq 0 \\ \Rightarrow & \left(\hat{\mathbf{h}}_I + \mathbf{e}_I \right) \mathbf{U}_I \left(\hat{\mathbf{h}}_I + \mathbf{e}_I \right)^H - \sigma^2 \geq 0 \\ \Rightarrow & \mathbf{e}_I \mathbf{U}_I \mathbf{e}_I^H + \mathbf{e}_I \left(\mathbf{U}_I \hat{\mathbf{h}}_I^H \right) + \left(\mathbf{U}_I \hat{\mathbf{h}}_I^H \right)^H \mathbf{e}_I^H + \hat{\mathbf{h}}_I \mathbf{U}_I \hat{\mathbf{h}}_I^H \\ & - \sigma^2 \geq 0 \end{aligned} \quad (54)$$

Lemma: S-procedure [43]: For a complex Hermitian matrix $\mathbf{U} \in \mathcal{C}^{N_t \times N_t}$, $\mathbf{b} \in \mathcal{C}^{N_t \times 1}$, a scalar c and a vector $\mathbf{v} \in \mathcal{C}^{1 \times N_t}$, the following condition

$$\mathbf{v} \mathbf{U} \mathbf{v}^H + \mathbf{v} \mathbf{b} + \mathbf{b}^H \mathbf{v}^H + c \geq 0, \quad \forall \|\mathbf{v}\|^2 \leq r^2 \quad (55)$$

is true if and only if there exists a non-negative variable t such that

$$\begin{bmatrix} \mathbf{U} + t \cdot \mathbf{I} & \mathbf{b} \\ \mathbf{b}^H & c - tr^2 \end{bmatrix} \succeq 0. \quad (56)$$

Subsequently, by employing the S-procedure into (54), the worst-case SINR constraint can be transformed into a positive semi-definite (PSD) form as

$$\begin{bmatrix} \mathbf{U}_I + t_I \cdot \mathbf{I} & \mathbf{U}_I \hat{\mathbf{h}}_I^H \\ \hat{\mathbf{h}}_I \mathbf{U}_I^H & \hat{\mathbf{h}}_I \mathbf{U}_I \hat{\mathbf{h}}_I^H - \sigma^2 - t_I \delta_0^2 \end{bmatrix} \succeq 0. \quad (57)$$

The worst-case energy constraint for the EH receiver k can be similarly transformed into a PSD form, given by

$$\begin{bmatrix} \gamma_0 \mathbf{U}_I + t_E^k \cdot \mathbf{I} & \gamma_0 \mathbf{U}_I \left(\hat{\mathbf{h}}_E^k \right)^H \\ \gamma_0 \hat{\mathbf{h}}_E^k \mathbf{U}_I^H & \gamma_0 \hat{\mathbf{h}}_E^k \mathbf{U}_I \left(\hat{\mathbf{h}}_E^k \right)^H - \frac{E_0}{\eta} - \sigma^2 - t_E^k \delta_0^2 \end{bmatrix} \succeq 0. \quad (58)$$

In (57) and (58), $t_I \geq 0$ and each $t_E^k \geq 0, \forall k \in \mathcal{K}$ are introduced auxiliary variables. Then, by defining $\hat{\mathbf{F}}_I = \hat{\mathbf{f}}_I \hat{\mathbf{f}}_I^H$, \mathcal{P}_9 can be transformed into an SDP as

$$\begin{aligned} \mathcal{P}_{10} : \quad & \min_{\hat{\mathbf{F}}_I} p \\ \text{s.t.} \quad & t_I \geq 0, t_E^k \geq 0, \forall k \in \mathcal{K} \\ & p \geq \text{tr} \left\{ \hat{\mathbf{F}}_{RF} \hat{\mathbf{F}}_I \hat{\mathbf{F}}_{RF}^H \right\} \\ & \mathbf{U}_I = \frac{1}{\gamma_0} \hat{\mathbf{F}}_{RF} \hat{\mathbf{F}}_I \hat{\mathbf{F}}_{RF}^H, \hat{\mathbf{F}}_I \succeq 0, \text{rank} \left\{ \hat{\mathbf{F}}_I \right\} = 1 \\ & \begin{bmatrix} \mathbf{U}_I + t_I \cdot \mathbf{I} & \mathbf{U}_I \hat{\mathbf{h}}_I^H \\ \hat{\mathbf{h}}_I \mathbf{U}_I^H & \hat{\mathbf{h}}_I \mathbf{U}_I \hat{\mathbf{h}}_I^H - \sigma^2 - t_I \delta_0^2 \end{bmatrix} \succeq 0 \\ & \begin{bmatrix} \gamma_0 \mathbf{U}_I + t_E^k \cdot \mathbf{I} & \gamma_0 \mathbf{U}_I \left(\hat{\mathbf{h}}_E^k \right)^H \\ \gamma_0 \hat{\mathbf{h}}_E^k \mathbf{U}_I^H & \gamma_0 \hat{\mathbf{h}}_E^k \mathbf{U}_I \left(\hat{\mathbf{h}}_E^k \right)^H - \frac{E_0}{\eta} - \sigma^2 - t_E^k \delta_0^2 \end{bmatrix} \succeq 0, \forall k \end{aligned} \quad (59)$$

Then, with $\hat{\mathbf{F}}_{RF}$ obtained by the SVD in Section IV or Algorithm 1 in Section V, \mathcal{P}_{10} can then be efficiently solved by dropping the rank-1 constraints. The robust solution for the hybrid iterative scheme can then be obtained by substituting \mathcal{P}_{10} with \mathcal{P}_5 in Algorithm 2.

VII. NUMERICAL RESULTS

A. Power Consumption Model at the BS

Before presenting the numerical results, to demonstrate the significant power savings introduced by the hybrid analog-digital architectures, we first introduce the power consumption model employed in the simulations. For the fully-digital case, the analog phase shifters are not needed. Then, based on [53][54], the power consumption model at the BS is given by

$$\begin{aligned} P_{BS}^D &= N_t(N_t + 1) P_{PA} + P_{BB} + N_t(P_{RFC} + P_{DAC}), \\ P_{BS}^F &= N_t(N_{RF}^t + 1) P_{PA} + N_t N_{RF}^t P_{PS} + P_{BB} \\ &\quad + N_{RF}^t(P_{RFC} + P_{DAC}), \\ P_{BS}^P &= N_t P_{PA} + N_t P_{PS} + P_{BB} + N_{RF}^t(P_{RFC} + P_{DAC}), \end{aligned} \quad (60)$$

where P_{BS}^D , P_{BS}^F , and P_{BS}^P denote the total power consumption at the BS for fully-digital case, hybrid fully-connected and hybrid partially-connected structures, respectively. In (60), $P_{PA} = (1/\eta_0) P_{TX}$ is the power consumed at the power amplifier to generate the transmit power P_{TX} , with η_0 being the power amplifier efficiency. P_{PS} represents the power consumption for phase shifters, P_{RFC} the power consumption for the RF chains, P_{DAC} the power consumption for the digital-to-analog converters, and P_{BB} the power consumption for the baseband processing. The value of the power consumption for each hardware component follows [53], which employs practical power values. This means that the power compensation for the losses existing in practical hardware components has already been taken into account. The simulation parameters are summarized in Table IV, and remain constant throughout the simulations unless otherwise stated. We further note that for the considered power minimization problem, the improved energy efficiency is obtained by requiring a lower total power consumption at the BS for a given performance.

Simulation parameters	Values
Antenna Number at the BS, N_t	12
Number of ID	1
Number of EH receivers, K	3
Number of RF chains, N_{RF}^t	4
Propagation constant, α_0	1
Pathloss coefficient, β	2
Shadow fading, C_I, C_E^k	1
Distance of ID and BS, D_I (m)	10
Distance of EH receivers and BS, D_E^k (m)	5
Channel noise power, σ^2 (mW)	0.1
Energy transfer efficiency, η	0.35
Power amplifier efficiency, η_0	0.5
Power of phase shifters, P_{PS} (mW)	30
Power of RF chains, P_{RFC} (mW)	40
Power of DAC, P_{DAC} (mW)	200
Power of baseband processing, P_{BB} (mW)	5
Channel uncertainty coefficient, δ_0	0.02

TABLE IV: Simulation Parameters

B. Results

In this section, we conduct Monte Carlo simulations to evaluate the performance of the proposed hybrid schemes. We compare our proposed schemes with the fully-digital scheme, and we further include a result for hybrid beamforming where analog beamformer employs random phases. The following abbreviations are applied for clarity:

- 1) ‘‘Fully-digital’’: conventional fully-digital scheme at the BS, \mathcal{P}_2 ;
- 2) ‘‘SVD, Fully/Partially’’: the proposed hybrid scheme based on the SVD in Section IV for the fully- and partially-connected structures respectively;
- 3) ‘‘Iterative, Fully/Partially’’: the proposed iterative hybrid design by Algorithm 2 in Section V for the fully- and partially-connected structures respectively;
- 4) ‘‘Random, Fully/Partially’’: the hybrid beamforming with an analog beamforming where the phase shifters employ random phases.

In Fig. 5, we evaluate the convergence of the proposed iterative scheme by plotting the value of the transmit power and the value of Δ with respect to the iteration number n . We select \mathbf{F}_{BB}^0 as the digital beamformer obtained by \mathcal{P}_5 in Section IV. It can be observed that the proposed iterative scheme is convergent within $n = 4$ iterations. Furthermore, the performance gap compared to the fully-digital case is marginal.

Fig. 6 presents the required transmit power P_{TX} and total power consumption at the BS P_{BS} of each scheme with respect to the increasing SINR target of the ID, where the harvested energy requirement for each EH receiver is $E_0 = 5\text{mW}$. Among hybrid structures, as expected the hybrid beamforming with random phases achieves the worst performance, as the analog beamformer does not exploit the channel. In terms of the required transmit power, the fully-digital case is the optimal and requires the lowest transmit power because of the full-RF structure, while the hybrid structures are sub-optimal and require a higher transmit power due to the reduced hard-

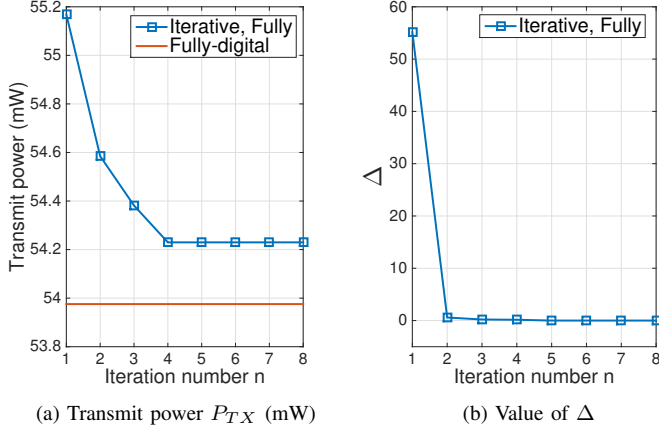


Fig. 5: Convergence of the iterative scheme for $N_t = 12$, one ID, $K = 3$ EH receivers, $E_0 = 5\text{mW}$, $\gamma_0 = 10\text{dB}$

ware components and the consequent reduced capability. More importantly, when we consider the total power required at the BS, on the contrary, the hybrid structures are indeed more advantageous. Thanks to the reduced number of RF chains, both hybrid structures are shown to significantly reduce the total power consumption required at the BS, which reveals that the hybrid structures are more energy efficient. In particular, the partially-connected structures are the most power efficient because of the reduced number of phase shifters, compared to the fully-connected structures.

In Fig. 7, we compare the required transmit power and the total power at the BS with an increasing harvested energy requirement for each EH receiver, where the SINR target for the ID is $\gamma_0 = 10\text{dB}$. It can be observed that both the transmit power and the total power consumption at the BS keep increasing with the increase in the harvested energy requirement E_0 . In both figures, the proposed iterative scheme outperforms the hybrid scheme based on SVD, and the per-

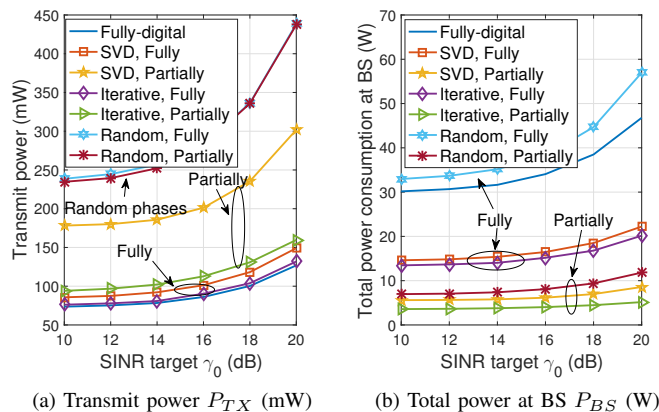


Fig. 6: Transmit power P_{TX} and total power at the BS P_{BS} required for $N_t = 12$, one ID, $K = 3$ EH receivers, $E_0 = 5\text{mW}$, $N_{max} = 4$

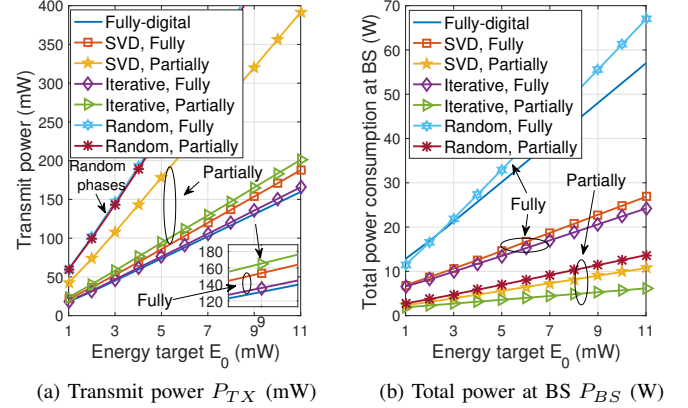


Fig. 7: Transmit power P_{TX} and total power at the BS P_{BS} required for $N_t = 12$, one ID, $K = 3$ EH receivers, $\gamma_0 = 10\text{dB}$, $N_{max} = 4$

formance gain is more significant for the partially-connected structures due to the optimal analog beamforming design. In Fig. 7 (b), it is shown that the iterative hybrid scheme with partially-connected structures requires the lowest total power consumption at the BS.

In Fig. 8, we compare the performance of the hybrid schemes with respect to the number of RF chains. With a reduced number of RF chains, the performance gap between the fully-digital case and hybrid structures is larger, and the proposed iterative hybrid scheme is shown to be less sensitive to the reduction in the number of RF chains. It is also observed that the performance gains of the proposed iterative scheme over the low-complexity hybrid scheme are more significant with a smaller number of RF chains. In Fig. 8 (b), we note that the total power consumption at the BS is jointly decided by the transmit power in Fig. 8 (a) and the number of RF chains, where the proposed iterative scheme still outperforms

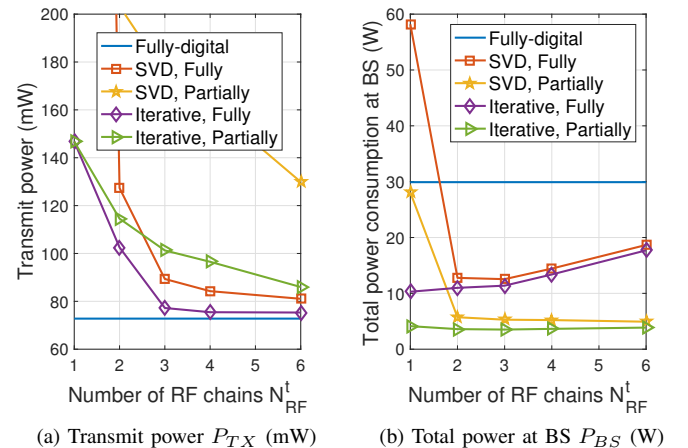


Fig. 8: Transmit power P_{TX} and total power at the BS P_{BS} required for $N_t = 12$, one ID, $K = 3$ EH receivers, $\gamma_0 = 10\text{dB}$, $N_{max} = 4$

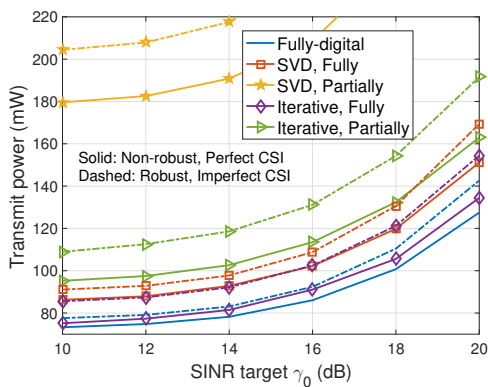


Fig. 9 Transmit power P_{TX} of the robust scheme for imperfect CSI, $N_t = 12$, one ID, $K = 3$ EH receivers, $E_0 = 5$ mW, $N_{max} = 4$, $\delta_0 = 0.02$

the low-complexity hybrid scheme based on SVD.

In Fig. 9, the required transmit power for the robust beamforming schemes for imperfect CSI is shown with the increasing SINR target of the ID, where the harvested energy requirement for each EH receiver is $E_0 = 5$ mW. It can be observed that compared to the perfect CSI case, the robust schemes require a higher transmit power to ensure that the SINR target and the energy requirements are met by considering the worst-case received SINR of the ID and harvested energy of each EH receiver. While the schemes for perfect CSI consume less power, they cannot guarantee that all the constraints are satisfied under the scenarios with imperfect CSI.

VIII. CONCLUSION

In this paper, the energy-efficient SWIPT techniques for MIMO systems with limited RF chains are studied, where we consider the scenario of one ID and several separate EH receivers. By analytically proving that in the scenario under study only an information beamformer is required, we propose a hybrid beamforming scheme based on SVD, followed by an iterative hybrid scheme that exploits this observation. We further propose the robust hybrid beamforming for imperfect CSI scenarios. It is shown that the hybrid structures require much less power to achieve the same performance as the fully-digital case, which makes the hybrid structures promising for the future energy-efficient transmission.

APPENDIX A PROOF OF PROPOSITION 1

In this case, the harvested energy by the information beamformer can already meet the energy requirement for the EH receiver, and therefore we have

$$\eta (\mathbf{h}_E \mathbf{w}_I \mathbf{w}_I^H \mathbf{h}_E^H + \sigma^2) > E_0, \quad (61)$$

and $\mathbf{w}_E^* = \mathbf{0}$ because in this case the presence of the energy beamformer will only degrade the received SINR performance of the ID. Based on the complementary slackness condition in

(8d), we further obtain $\lambda_I > 0$ and $\lambda_E = 0$. Accordingly, the KKT conditions can be simplified into

$$\mathbf{w}_I^H - \frac{\lambda_I}{\gamma_0} \mathbf{w}_I^H \mathbf{h}_I^H \mathbf{h}_I = \mathbf{0}, \quad \sigma^2 - \frac{1}{\gamma_0} \mathbf{h}_I \mathbf{w}_I \mathbf{w}_I^H \mathbf{h}_I^H = 0. \quad (62)$$

We note that the optimal \mathbf{w}_I is not unique and is invariant to a phase rotation, and therefore in (62) we can assume there exists an optimal \mathbf{w}_I such that $\Im \{\mathbf{h}_I \mathbf{w}_I\} = \Im \{\mathbf{w}_I^H \mathbf{h}_I^H\} = 0$, which leads to

$$\mathbf{h}_I \mathbf{w}_I = \mathbf{w}_I^H \mathbf{h}_I^H = \sqrt{\gamma_0 \sigma^2}. \quad (63)$$

We can further obtain $\lambda_I = \frac{\gamma_0}{(\mathbf{h}_I \mathbf{h}_I^H)}$, which leads to the final expression of the optimal \mathbf{w}_I , given by

$$\mathbf{w}_I^* = \frac{\sqrt{\gamma_0 \sigma^2}}{(\mathbf{h}_I \mathbf{h}_I^H)} \cdot \mathbf{h}_I^H. \quad (64)$$

Subsequently, we obtain the optimal transmit power as

$$P_{TX}^* = (\mathbf{w}_I^*)^H \mathbf{w}_I^* = \frac{\gamma_0 \sigma^2}{(\mathbf{h}_I \mathbf{h}_I^H)}, \quad (65)$$

which is only relevant to the SINR target of the ID and not relevant to E_0 . Based on (61), the harvested energy requirement should satisfy

$$\begin{aligned} \frac{E_0}{\eta} - \sigma^2 &\leq \mathbf{h}_E \mathbf{w}_I \mathbf{w}_I^H \mathbf{h}_E^H \\ \Rightarrow E_0 &\leq \frac{\gamma_0 \eta \sigma^2 (\mathbf{h}_I \mathbf{h}_I^H \mathbf{h}_E \mathbf{h}_E^H)}{(\mathbf{h}_I \mathbf{h}_I^H)^2} + \eta \sigma^2 \triangleq E_{th}^1. \end{aligned} \quad (66)$$

APPENDIX B PROOF OF PROPOSITION 2

In this case, the SINR requirement for the ID is over-satisfied, and we have

$$\frac{1}{\gamma_0} \mathbf{h}_I \mathbf{w}_I \mathbf{w}_I^H \mathbf{h}_I^H > \mathbf{h}_I \mathbf{w}_E \mathbf{w}_E^H \mathbf{h}_I^H + \sigma^2. \quad (67)$$

Based on the complementary slackness condition in (8c), we then have $\lambda_I = 0$ and $\lambda_E > 0$, and the stationarity conditions in (8a) and (8b) can be further transformed into

$$\mathbf{w}_I^H - \lambda_E \mathbf{w}_I^H \mathbf{h}_E^H \mathbf{h}_E = \mathbf{w}_I^H (\mathbf{I} - \lambda_E \mathbf{h}_E^H \mathbf{h}_E) = \mathbf{0} \quad (68a)$$

$$\mathbf{w}_E^H - \lambda_E \mathbf{w}_E^H \mathbf{h}_E^H \mathbf{h}_E = \mathbf{w}_E^H (\mathbf{I} - \lambda_E \mathbf{h}_E^H \mathbf{h}_E) = \mathbf{0} \quad (68b)$$

It is observed that the optimal \mathbf{w}_I and \mathbf{w}_E are parallel, and without loss of generality we can assume

$$\mathbf{w}_E = c \cdot \mathbf{w}_I, \quad (69)$$

where $c \geq 0$. Furthermore, as the energy constraint is active, we substitute (23) into (8d), which yields

$$\begin{aligned} (1 + c^2) \mathbf{h}_E \mathbf{w}_I \mathbf{w}_I^H \mathbf{h}_E^H &= \frac{E_0}{\eta} - \sigma^2 \\ \Rightarrow \mathbf{h}_E \mathbf{w}_I &= \mathbf{w}_I^H \mathbf{h}_E^H = \sqrt{\frac{E_0 - \eta \sigma^2}{\eta (1 + c^2)}}. \end{aligned} \quad (70)$$

By substituting (70) into (68a), the optimal information beamformer and energy beamformer can be obtained as

$$\mathbf{w}_I^* = \frac{\sqrt{\frac{E_0 - \eta \sigma^2}{\eta (1 + c^2)}}}{(\mathbf{h}_E \mathbf{h}_E^H)} \cdot \mathbf{h}_E^H, \quad \mathbf{w}_E^* = \frac{c \sqrt{\frac{E_0 - \eta \sigma^2}{\eta (1 + c^2)}}}{(\mathbf{h}_E \mathbf{h}_E^H)} \cdot \mathbf{h}_E^H. \quad (71)$$

By further incorporating the expressions of the optimal beamforming vectors into (67), we can obtain

$$\frac{\frac{E_0 - \eta\sigma^2}{\gamma_0\eta(1+c^2)}}{(\mathbf{h}_E\mathbf{h}_E^H)^2} (\mathbf{h}_I\mathbf{h}_E^H\mathbf{h}_E\mathbf{h}_I^H) > c^2 \frac{\frac{E_0 - \eta\sigma^2}{\eta(1+c^2)}}{(\mathbf{h}_E\mathbf{h}_E^H)^2} (\mathbf{h}_I\mathbf{h}_E^H\mathbf{h}_E\mathbf{h}_I^H) + \sigma^2. \quad (72)$$

With some further transformations based on (72), we obtain that c should satisfy

$$\begin{aligned} \frac{1}{\gamma_0} &> c^2 + \frac{(1+c^2)\eta\sigma^2(\mathbf{h}_E\mathbf{h}_E^H)^2}{(E_0 - \eta\sigma^2)(\mathbf{h}_I\mathbf{h}_E^H\mathbf{h}_E\mathbf{h}_I^H)} \\ \Rightarrow c^2 &< \frac{1}{\gamma_0} \cdot \frac{(E_0 - \eta\sigma^2)(\mathbf{h}_I\mathbf{h}_E^H\mathbf{h}_E\mathbf{h}_I^H) - \gamma_0\eta\sigma^2(\mathbf{h}_E\mathbf{h}_E^H)^2}{(E_0 - \eta\sigma^2)(\mathbf{h}_I\mathbf{h}_E^H\mathbf{h}_E\mathbf{h}_I^H) + \eta\sigma^2(\mathbf{h}_E\mathbf{h}_E^H)^2}. \end{aligned} \quad (73)$$

Since $c^2 \geq 0$, based on (73) we can obtain the requirement for E_0 , which is given by

$$E_0 \geq \frac{\gamma_0\eta\sigma^2(\mathbf{h}_E\mathbf{h}_E^H)^2}{(\mathbf{h}_I\mathbf{h}_E^H\mathbf{h}_E\mathbf{h}_I^H)} + \eta\sigma^2 \triangleq E_{th}^2, \quad (74)$$

and we further note that E_{th}^2 obtained in (74) is guaranteed to be larger than E_{th}^1 in (66) based on the inner-product property, where we have

$$\mathbf{h}_I\mathbf{h}_I^H\mathbf{h}_E\mathbf{h}_E^H \geq \mathbf{h}_I\mathbf{h}_E^H\mathbf{h}_E\mathbf{h}_I^H. \quad (75)$$

In (75), the equality holds only when \mathbf{h}_I and \mathbf{h}_E are parallel. Subsequently, we obtain the optimal transmit power as

$$P_{TX}^* = (1+c^2)(\mathbf{w}_I^*)^H \mathbf{w}_I^* = \frac{E_0 - \eta\sigma^2}{\eta(\mathbf{h}_E\mathbf{h}_E^H)}, \quad (76)$$

which is independent of c .

APPENDIX C PROOF OF PROPOSITION 3

We firstly derive the expression of the total transmit power, based on which we prove that $\mathbf{w}_E^* = \mathbf{0}$ by contradiction. We then obtain the expression of the optimal information beamformer \mathbf{w}_I^* . To be specific, we multiply \mathbf{w}_I and \mathbf{w}_E to the right-hand side of (8a) and (8b) respectively, and we can further obtain

$$\mathbf{w}_I^H \mathbf{w}_I = \frac{\lambda_I}{\gamma_0} \mathbf{h}_I \mathbf{w}_I \mathbf{w}_I^H \mathbf{h}_I^H + \lambda_E \mathbf{h}_E \mathbf{w}_I \mathbf{w}_I^H \mathbf{h}_E^H \quad (77a)$$

$$\mathbf{w}_E^H \mathbf{w}_E = -\lambda_I \mathbf{h}_I \mathbf{w}_E \mathbf{w}_E^H \mathbf{h}_I^H + \lambda_E \mathbf{h}_E \mathbf{w}_E \mathbf{w}_E^H \mathbf{h}_E^H \quad (77b)$$

The sum of (77a) and (77b) yields

$$\begin{aligned} \mathbf{w}_I^H \mathbf{w}_I + \mathbf{w}_E^H \mathbf{w}_E &= \lambda_I \left(\frac{1}{\gamma_0} \mathbf{h}_I \mathbf{w}_I \mathbf{w}_I^H \mathbf{h}_I^H - \mathbf{h}_I \mathbf{w}_E \mathbf{w}_E^H \mathbf{h}_I^H \right) \\ &\quad + \lambda_E (\mathbf{h}_E \mathbf{w}_I \mathbf{w}_I^H \mathbf{h}_E^H + \mathbf{h}_E \mathbf{w}_E \mathbf{w}_E^H \mathbf{h}_E^H). \end{aligned} \quad (78)$$

It is observed in (78) that the left-hand side is the total transmit power. Since both the SINR constraint and the energy constraint are active, the right-hand side can be further simplified and the total transmit power is obtained as

$$P_{TX}^* = \lambda_I \sigma^2 + \lambda_E \left(\frac{E_0}{\eta} - \sigma^2 \right), \quad (79)$$

which means that the optimal transmit power is only related to the dual variables.

Based on (79), we proceed to prove that $\mathbf{w}_E^* = \mathbf{0}$ by contradiction. We firstly assume one case where the optimal solution is an information beamformer \mathbf{w}_I^0 only that satisfies both of the constraints, and the corresponding power consumption is obtained as

$$P_{TX}^0 = \lambda_I^0 \sigma^2 + \lambda_E^0 \left(\frac{E_0}{\eta} - \sigma^2 \right). \quad (80)$$

In addition, we consider another case where we need an information beamformer \mathbf{w}_I and an energy beamformer \mathbf{w}_E to satisfy both of the constraints with the same total transmit power. The total power consumption in this case is expressed as

$$P_{TX} = \lambda_I \sigma^2 + \lambda_E \left(\frac{E_0}{\eta} - \sigma^2 \right). \quad (81)$$

As can be observed, to have $P_{TX} = P_{TX}^0$, we can obtain $\lambda_I = \lambda_I^0$ and $\lambda_E = \lambda_E^0$. Then, we express the stationarity condition for \mathbf{w}_I^0 and \mathbf{w}_I as

$$(\mathbf{w}_I^0)^H \left(\mathbf{I} - \frac{\lambda_I^0}{\gamma_0} \mathbf{h}_I \mathbf{h}_I^H - \lambda_E^0 \mathbf{h}_E \mathbf{h}_E^H \right) = \mathbf{0}, \quad (82a)$$

$$\mathbf{w}_I^H \left(\mathbf{I} - \frac{\lambda_I}{\gamma_0} \mathbf{h}_I \mathbf{h}_I^H - \lambda_E \mathbf{h}_E \mathbf{h}_E^H \right) = \mathbf{0}. \quad (82b)$$

With $\lambda_I = \lambda_I^0$ and $\lambda_E = \lambda_E^0$, it is then observed that \mathbf{w}_I^0 and \mathbf{w}_I are parallel, and without loss of generality we assume

$$\mathbf{w}_I = a \cdot \mathbf{w}_I^0, \quad (83)$$

where a is real and $a \neq 0$. As the SINR constraint is active for both cases, we can obtain

$$\frac{1}{\gamma_0} \mathbf{h}_I \mathbf{w}_I^0 (\mathbf{w}_I^0)^H \mathbf{h}_I^H = \sigma^2, \quad (84)$$

$$\frac{a^2}{\gamma_0} \mathbf{h}_I \mathbf{w}_I^0 (\mathbf{w}_I^0)^H \mathbf{h}_I^H = \mathbf{h}_I \mathbf{w}_E \mathbf{w}_E^H \mathbf{h}_I^H + \sigma^2.$$

(84) can be further transformed into

$$\frac{(a^2 - 1)}{\gamma_0} \mathbf{h}_I \mathbf{w}_I^0 (\mathbf{w}_I^0)^H \mathbf{h}_I^H = \mathbf{h}_I \mathbf{w}_E \mathbf{w}_E^H \mathbf{h}_I^H. \quad (85)$$

Since $\mathbf{w}_E \neq \mathbf{0}$, we have $a^2 > 1$. On the other hand, by considering the active energy constraint, similarly we will obtain $a^2 < 1$ to satisfy the energy constraint, which causes contradiction. Therefore, the optimal case is to employ the information beamformer only.

When both of the SINR and harvested energy constraints are active, it is difficult to compute the exact closed-form expression of \mathbf{w}_I^* . Nevertheless, based on the observation that both of the SINR and energy constraints are active with the increasing E_0 when $E_0 \in [E_{th}^1, E_{th}^2]$, we can obtain that the optimal beamforming vector \mathbf{w}_I is in the form of [55]

$$\mathbf{w}_I = \alpha \cdot \mathbf{h}_I^H + \beta \cdot \mathbf{h}_\perp^H, \quad (86)$$

where \mathbf{h}_\perp is orthogonal to \mathbf{h}_I and can be expressed as $\mathbf{h}_\perp = \mathbf{h}_E - \frac{\mathbf{h}_E \mathbf{h}_I^H \mathbf{h}_I}{(\mathbf{h}_I \mathbf{h}_I^H)}$. In (86), α can be chosen as $\alpha = \frac{\sqrt{\gamma_0 \sigma^2}}{(\mathbf{h}_I \mathbf{h}_I^H)}$. This structure ensures that the SINR constraint is met, and the value of the complex weighting factor β dependent on E_0 can be obtained with the active energy harvesting constraint.

REFERENCES

- [1] D. W. K. Ng, E. S. Lo, and R. Schober, "Wireless Information and Power Transfer: Energy Efficiency Optimization in OFDMA Systems," *IEEE Trans. Wireless Commun.*, vol. 12, no. 2, pp. 6352–6370, Dec. 2013.
- [2] T. Chen, Y. Yang, H. Zhang, H. Kim, and K. Horneman, "Network Energy Saving Technologies for Green Wireless Access Networks," *IEEE Trans. Wireless Commun.*, vol. 18, no. 5, pp. 30–38, Oct. 2011.
- [3] K. Pentikousis, "In Search of Energy-Efficient Mobile Networking," *IEEE Commun. Mag.*, vol. 48, no. 1, pp. 95–103, Jan. 2010.
- [4] S. Sudevalayam and P. Kulkarni, "Energy Harvesting Sensor Nodes: Survey and Implications," *IEEE Commun. Surveys. Tut.*, vol. 13, no. 3, pp. 443–461, 3rd Quart. 2011.
- [5] G. Monti, L. Corchia, and L. Tarricone, "UHF Wearable Rectenna on Textile Materials," *IEEE Trans. Ant. Propag.*, vol. 61, no. 7, pp. 3869–3873, July 2013.
- [6] U. Olgun, C.-C. Chen, and J. L. Volakis, "Investigation of Rectenna Array Configurations for Enhanced RF Power Harvesting," *IEEE Ant. Wireless Propag. Lett.*, vol. 10, pp. 262–265, 2011.
- [7] W. Ejaz, M. Naeem, M. Basharat, A. Anpalagan, and S. Kandeepan, "Efficient Wireless Power Transfer in Software-Defined Wireless Sensor Networks," *IEEE Sensors Journal*, vol. 16, no. 20, pp. 7409–7420, Oct. 2016.
- [8] Z. Wang, L. Duan, and R. Zhang, "Adaptively Directional Wireless Power Transfer for Large-Scale Sensor Networks," *IEEE J. Sel. Areas Commun.*, vol. 34, no. 5, pp. 1785–1800, May 2016.
- [9] Y.-W. P. Hong, T.-C. Hsu, and P. Chennakesavula, "Wireless Power Transfer for Distributed Estimation in Wireless Passive Sensor Networks," *IEEE Trans. Sig. Process.*, vol. 64, no. 20, pp. 5382–5395, Oct. 2016.
- [10] S. Bi, Y. Zeng, and R. Zhang, "Wireless Powered Communication Networks: An Overview," *IEEE Wireless Commun.*, vol. 23, no. 2, pp. 10–18, May 2016.
- [11] V. Chawla and D. S. Ha, "An Overview of Passive RFID," *IEEE Commun. Mag.*, vol. 45, no. 9, pp. 11–17, Sept. 2007.
- [12] L. Varshney, "Transporting Information and Energy Simultaneously," in *2008 IEEE International Symposium on Information Theory*, Toronto, ON, 2008, pp. 1612–1616.
- [13] P. Grover and A. Sahai, "Shannon Meets Tesla: Wireless Information and Power Transfer," in *2010 IEEE International Symposium on Information Theory*, Austin, TX, 2010, pp. 2363–2367.
- [14] R. Zhang and C. K. Ho, "MIMO Broadcasting for Simultaneous Wireless Information and Power Transfer," *IEEE Trans. Wireless Commun.*, vol. 12, no. 5, pp. 1989–2001, May 2013.
- [15] Z. Ding, C. Zhong, D. W. K. Ng, M. Peng, H. A. Suraweera, R. Schober, and H. V. Poor, "Application of Smart Antenna Technologies in Simultaneous Wireless Information and Power Transfer," *IEEE Commun. Mag.*, vol. 53, no. 4, pp. 86–93, April 2015.
- [16] T. L. Thanh, M. D. Renzo, and J. P. Coon, "MIMO Cellular Networks with Simultaneous Wireless Information and Power Transfer," in *2016 IEEE 17th International Workshop on Signal Processing Advances in Wireless Communications (SPAWC)*, Edinburgh, 2016, pp. 1–5.
- [17] M. Sheng, L. Wang, X. Wang, Y. Zhang, C. Xu, and J. Li, "Energy Efficient Beamforming in MISO Heterogeneous Cellular Networks with Wireless Information and Power Transfer," *IEEE J. Sel. Areas Commun.*, vol. 34, no. 4, pp. 954–968, April 2016.
- [18] A. Ozcelikkale, T. McKelvey, and M. Viberg, "Wireless Information and Power Transfer in MIMO Channels under Rician Fading," in *2015 IEEE International Conference on Acoustics, Speech and Signal Processing (ICASSP)*, South Brisbane, QLD, 2015, pp. 3187–3191.
- [19] H. Son and B. Clerckx, "Joint Beamforming Design for Multi-User Wireless Information and Power Transfer," *IEEE Trans. Wireless Commun.*, vol. 13, no. 11, pp. 6397–6409, Aug. 2014.
- [20] J. Xu, L. Liu, and R. Zhang, "Multiuser MISO Beamforming for Simultaneous Wireless Information and Power Transfer," *IEEE Trans. Sig. Process.*, vol. 62, no. 18, pp. 4798–4810, Sept. 2014.
- [21] S. Timotheou, G. Zheng, C. Masouros, and I. Krikidis, "Exploiting Constructive Interference for Simultaneous Wireless Information and Power Transfer in Multiuser Downlink Systems," *IEEE J. Sel. Areas Commun.*, vol. 34, no. 5, pp. 1772–1784, May 2016.
- [22] Z. Zong, H. Feng, F. R. Yu, N. Zhao, T. Yang, and B. Hu, "Optimal Transceiver Design for SWIPT in K-User MIMO Interference Channels," *IEEE Trans. Wireless Commun.*, vol. 15, no. 1, pp. 430–445, Jan. 2016.
- [23] S. Lee, L. Liu, and R. Zhang, "Collaborative Wireless Energy and Information Transfer in Interference Channel," *IEEE Trans. Wireless Commun.*, vol. 14, no. 1, pp. 545–557, Sept. 2015.
- [24] J. Park and B. Clerckx, "Joint Wireless Information and Energy Transfer in a K-User MIMO Interference Channel," *IEEE Trans. Wireless Commun.*, vol. 13, no. 10, pp. 5781–5796, Oct. 2014.
- [25] J. Xiao, C. Xu, X. Huang, and J. Qin, "Robust Transceiver Design for Two-User MIMO Interference Channel with Simultaneous Wireless Information and Power Transfer," *IEEE Trans. Veh. Tech.*, vol. 65, no. 5, pp. 3823–3828, May 2016.
- [26] N. Zhao, F. R. Yu, and V. C. M. Leung, "Opportunistic Communications in Interference Alignment Networks with Wireless Power Transfer," *IEEE Wireless Commun.*, vol. 22, no. 1, pp. 88–95, Feb. 2015.
- [27] —, "Wireless Energy Harvesting in Interference Alignment Networks," *IEEE Commun. Mag.*, vol. 53, no. 6, pp. 72–78, June 2015.
- [28] J. Guo, N. Zhao, F. R. Yu, X. Liu, and V. C. M. Leung, "Exploiting adversarial jamming signals for energy harvesting in interference networks," *IEEE Trans. Wireless Commun.*, vol. 16, no. 2, pp. 1267–1280, Feb. 2017.
- [29] X. Chen, D. W. K. Ng, and H.-H. Chen, "Secrecy Wireless Information and Power Transfer: Challenges and Opportunities," *IEEE Wireless Commun.*, vol. 23, no. 2, pp. 54–61, May 2016.
- [30] Q. Shi, W. Xu, J. Wu, E. Song, and Y. Wang, "Secure Beamforming for MIMO Broadcasting with Wireless Information and Power Transfer," *IEEE Trans. Wireless Commun.*, vol. 14, no. 5, pp. 2841–2853, Jan. 2015.
- [31] X. Chen, J. Chen, and T. Liu, "Secure Transmission in Wireless Powered Massive MIMO Relaying Systems: Performance Analysis and Optimization," *IEEE Trans. Veh. Tech.*, vol. 65, no. 10, pp. 8025–8035, Oct. 2016.
- [32] S. Wang and B. Wang, "Robust Secure Transmit Design in MIMO Channels with Simultaneous Wireless Information and Power Transfer," *IEEE Sig. Process. Lett.*, vol. 22, no. 11, pp. 2147–2151, Nov. 2015.
- [33] O. E. Ayach, S. Rajagopal, S. Abu-Surra, Z. Pi, and R. W. Heath, "Spatially Sparse Precoding in Millimeter Wave MIMO Systems," *IEEE Trans. Wireless Commun.*, vol. 13, no. 3, pp. 1499–1513, Jan. 2014.
- [34] L. Liang, W. Xu, and X. Dong, "Low-Complexity Hybrid Precoding in Massive Multiuser MIMO Systems," *IEEE Wireless Commun. Lett.*, vol. 3, no. 6, pp. 653–656, Oct. 2014.
- [35] A. Li and C. Masouros, "Hybrid Analog-Digital mmWave MU-MIMO Transmission with Virtual Path Selection," *IEEE Commun. Lett.*, vol. 21, no. 2, pp. 438–441, Feb. 2017.
- [36] A. Garcia-Rodriguez, C. Masouros, and P. Rulikowski, "Reduced Switching Connectivity for Large Scale Antenna Selection," *IEEE Trans. Commun.*, vol. 65, no. 5, pp. 2250–2263, May 2017.
- [37] W. Ni and X. Dong, "Hybrid Block Diagonalization for Massive Multiuser MIMO Systems," *IEEE Trans. Commun.*, vol. 64, no. 1, pp. 201–211, Jan. 2016.
- [38] V. Venkateswaran, F. Pivit, and L. Guan, "Hybrid RF and Digital Beamformer for Cellular Networks: Algorithms, Microwave Architectures, and Measurements," *IEEE Trans. Microwave Theory and Techniques*, vol. 64, no. 7, pp. 2226–2243, July 2016.
- [39] A. Garcia-Rodriguez, V. Venkateswaran, P. Rulikowski, and C. Masouros, "Hybrid Analog-Digital Precoding Revisited Under Realistic RF Modeling," *IEEE Wireless Commun. Lett.*, vol. 5, no. 5, pp. 528–531, Oct. 2016.
- [40] S. Han, C.-I. I. Z. Xu, and C. Rowell, "Large-Scale Antenna Systems with Hybrid Analog and Digital Beamforming for Millimeter Wave 5G," *IEEE Commun. Mag.*, vol. 53, no. 1, pp. 186–194, Jan. 2015.
- [41] K. Yang, Q. Yu, S. Leng, B. Fan, and F. Wu, "Data and Energy Integrated Communication Networks for Wireless Big Data," *IEEE Access*, vol. 4, pp. 713–723, Feb. 2016.
- [42] Y. Zeng, B. Clerckx, and R. Zhang, "Communications and Signals Design for Wireless Power Transmission," *IEEE Trans. Commun.*, vol. 65, no. 5, pp. 2264–2290, May 2017.
- [43] S. Boyd and L. Vandenberghe, *Convex Optimization*. Cambridge University Press, 2004.
- [44] Y. Huang and D. Palomar, "Rank-Constrained Separable Semidefinite Programming with Applications to Optimal Beamforming," *IEEE Trans. Sig. Process.*, vol. 58, no. 2, pp. 664–678, Feb. 2010.
- [45] Z.-Q. Luo, W.-K. Ma, A. M.-C. So, Y. Ye, and S. Zhang, "Semidefinite Relaxation of Quadratic Optimization Problems: From Its Practical Deployments and Scope of Applicability to Key Theoretical Results," *IEEE Sig. Process. Mag.*, vol. 27, no. 3, pp. 20–34, May 2010.
- [46] M. Razaviyayn, M. Hong, and Z.-Q. Luo, "A Unified Convergence Analysis of Block Successive Minimization Methods for Nonsmooth Optimization," *SIAM J. Optim.*, vol. 23, no. 2, pp. 1126–1153, 2013.

- [47] Q. Zhang, C. He, and L. Jiang, "Per-Stream MSE based Linear Transceiver Design for MIMO Interference Channels with CSI Error," *IEEE Trans. Commun.*, vol. 63, no. 5, pp. 1676–1689, 2015.
- [48] A. Ben-Tal and A. Nemirovski, *Lectures on Modern Convex Optimization: Analysis, Algorithms, and Engineering Applications*. Philadelphia, PA, USA: Society for Industrial and Applied Mathematics, 2001.
- [49] A. Alkhateeb, O. E. Ayach, G. Leus, and R. W. Heath, "Channel Estimation and Hybrid Precoding for Millimeter Wave Cellular Systems," *IEEE J. Sel. Topics Sig. Process.*, vol. 8, no. 5, pp. 831–846, Oct. 2014.
- [50] Z. Gao, C. Hu, L. Dai, and Z. Wang, "Channel Estimation for Millimeter-Wave Massive MIMO with Hybrid Precoding over Frequency-Selective Fading Channels," *IEEE Commun. Lett.*, vol. 20, no. 6, pp. 1259–1262, June 2016.
- [51] L. Zhao, D. W. K. Ng, and J. Yuan, "Multi-User Precoding and Channel Estimation for Hybrid Millimeter Wave Systems," *IEEE J. Sel. Areas Commun.*, vol. 35, no. 7, pp. 1576–1590, July 2017.
- [52] J. Wang and D. Palomar, "Worst-Case Robust MIMO Transmission with Imperfect Channel Knowledge," *IEEE Trans. Sig. Process.*, vol. 57, no. 8, pp. 3086–3100, Aug. 2009.
- [53] R. Mendez-Rial, C. Rusu, N. Gonzalez-Prelcic, A. Alkhateeb, and R. W. Heath Jr., "Hybrid MIMO Architectures for Millimeter Wave Communications: Phase Shifters or Swithes?" *IEEE Access*, vol. 4, pp. 247–267, Jan. 2016.
- [54] C. Masouros, M. Sellathurai, and T. Ratnarajah, "Maximizing Energy Efficiency in the Vector Precoded MU-MISO Downlink by Selective Perturbation," *IEEE Trans. Wireless Commun.*, vol. 13, no. 9, pp. 4974–4984, Sept. 2014.
- [55] R. Zhang and Y.-C. Liang, "Exploiting Multi-Antennas for Opportunistic Spectrum Sharing in Cognitive Radio Networks," *IEEE J. Sel. Areas Commun.*, vol. 2, no. 1, pp. 88–102, Feb. 2008.



Ang Li (S'14) received the Bachelor and Master degree in Electronic and Information Engineering from Xi'an Jiaotong University in 2011 and 2014, respectively. He is currently pursuing the Ph.D. degree in the Communications and Information Systems research group, Dept. Electrical & Electronic Engineering, University College London. His research interests lie in the field of wireless communications with focus on beamforming designs for MIMO systems and mmWave communications.



Christos Masouros (M'06-SM'14) received the Diploma degree in Electrical and Computer Engineering from the University of Patras, Greece, in 2004, and MSc by research and PhD in Electrical and Electronic Engineering from the University of Manchester, UK in 2006 and 2009 respectively. In 2008 he was a research intern at Philips Research Labs, UK. Between 2009-2010 he was a Research Associate in the University of Manchester and between 2010-2012 a Research Fellow in Queen's University Belfast. He has held a Royal Academy

of Engineering Research Fellowship between 2011-2016.

He is currently a Senior Lecturer in the Communications and Information Systems research group, Dept. Electrical & Electronic Engineering, University College London. His research interests lie in the field of wireless communications and signal processing with particular focus on Green Communications, Large Scale Antenna Systems, Cognitive Radio, interference mitigation techniques for MIMO and multicarrier communications. He was the recipient of the Best Paper Award in the IEEE GlobeCom conference 2015, and has been recognised as an Exemplary Editor for the IEEE Communications Letters, and as an Exemplary Reviewer for the IEEE Transactions on Communications. He is an Associate Editor for IEEE Communications Letters, and Guest Editor for IEEE Journal on Selected Topics in Signal Processing issue "Exploiting Interference towards Energy Efficient and Secure Wireless Communications".